Organic & Biomolecular Chemistry

ROYAL SOCIETY OF CHEMISTRY

REVIEW

View Article Online
View Journal

Check for updates

Cite this: DOI: 10.1039/d6ob00343e

Recent advances in allylic and vinylic C–H bond functionalization of simple alkenes *via* visible-light photocatalysis

Etikala Ashok,[a] Junghwa Woo,[a] Juyoung Yang[a] and Jungwon Kim *[a,b]

Received 28th February 2026,
Accepted 11th May 2026

DOI: 10.1039/d6ob00343e

rsc.li/obc

The selective functionalization of allylic and vinylic C–H bonds in simple alkenes represents a powerful yet challenging strategy for the direct construction of value-added molecular architectures from readily available feedstocks. Traditional approaches to allylic and vinylic C–H bond activation often rely on harsh reaction conditions, stoichiometric oxidants, or transition-metal catalysts, limiting functional-group tolerance and sustainability. In recent years, visible-light photocatalysis has emerged as a mild and versatile platform for allylic and vinylic C–H bond functionalization *via* single-electron transfer, energy transfer, and hydrogen-atom-transfer pathways. This approach allows the controlled generation of several radical intermediates under ambient conditions, facilitating a broad range of transformations. In this review, recent advances in allylic and vinylic C–H bond functionalization are introduced together with representative examples. By organizing recent reports according to their underlying mechanistic pathways, this review aims to provide informative references and insights for further research on alkene functionalization *via* visible-light photocatalysis.

Open Access Article. Published on 18 May 2026. Downloaded on 5/26/2026 2:04:15 AM.
This article is licensed under a Creative Commons Attribution 3.0 Unported Licence.

1. Introduction

Alkenes are among the most important and versatile chemical building blocks in organic and industrial chemistry. This synthetic adaptability makes them key intermediates in multistep organic syntheses, particularly in the construction of complex molecules.[1] Furthermore, alkenes serve as fundamental mono-

[a]*Department of Chemistry (BK21 four), Gyeongsang National University, Jinju 52828, Republic of Korea. E-mail: jungwon.kim@gnu.ac.kr*
[b]*Research Institute of Advanced Chemistry, Gyeongsang National University, Jinju 52828, Republic of Korea*

Etikala Ashok

Etikala Ashok was born in Mallampally, Siddipet (Dist), Telangana, India. He obtained his M.S. degree in Organic Chemistry from Palamuru University. Afterwards, he completed his Ph.D. in 2024 at the University of Hyderabad under the supervision of Prof. D. B. Ramachary. Later that year, he joined Dr Reddy's Institute of Life Sciences on the University of Hyderabad campus as a postdoctoral researcher. In 2025, he moved to Sai Life Sciences Limited in Hyderabad as a Research Scientist. Currently, he is pursuing postdoctoral research at Gyeongsang National University, Republic of Korea. His research focuses on stereoselective synthesis via visible-light photocatalysis.

Junghwa Woo

Junghwa Woo was born in Changwon, Republic of Korea, in 2001. He received his B.S. degree in Chemistry from Gyeongsang National University in 2026. He is currently pursuing an M.S. degree in the Department of Chemistry at Gyeongsang National University under the supervision of Prof. Jungwon Kim. His research focuses on the regioselective hydrofunctionalization of alkenes via visible-light photocatalysis.

Open Access Article. Published on 18 May 2026. Downloaded on 5/26/2026 2:04:15 AM.
This article is licensed under a Creative Commons Attribution 3.0 Unported Licence.

mers in polymer chemistry, underpinning the large-scale production of plastics, elastomers, and advanced materials.[2] Their widespread availability, low cost, and accessibility from petrochemical feedstocks further reinforce their central role in industrial chemistry, including the synthesis of fuels, detergents, pharmaceuticals, and agrochemicals. Together, these attributes firmly establish alkenes as indispensable molecular scaffolds for modern chemical synthesis and materials science.

The Mizoroki–Heck reaction is a powerful cross-coupling method for forming substituted alkenes *via* direct C–C bond formation between aryl or vinyl halides and alkenes under mild conditions.[3] First reported in the early 1970s,[4] this transformation enabled predictable alkene formation *via* vinylic C(sp^2)–H bond functionalization. It exhibits high regio- and stereoselectivity, broad substrate scope, and excellent functional-group tolerance, making it a cornerstone of modern synthetic chemistry.[5] Alongside this cross-coupling strategy, allylic C(sp^3)–H functionalization has emerged as a highly attractive and atom-economical approach to alkene derivatization.[6] This strategy enables the direct conversion of simple alkenes into synthetically useful molecules through the selective activation of allylic C(sp^3)–H bonds, thereby minimizing step count and waste generation. Substantial progress in transition-metal catalysis—particularly palladium-,[7] iridium-,[8] rhodium-,[8] and copper-based systems[9]—has enabled allylic oxidation, amination, and substitution reactions with high levels of site- and chemoselectivity.

Despite the power of transition-metal catalysis for allylic and vinylic C(sp^2)–H bond functionalization, their broader synthetic utility remains limited. For example, the Mizoroki–Heck reaction inherently requires pre-functionalized halides, which generate stoichiometric salt waste, and are notorious for their inability to incorporate unactivated sp^3-hybridized alkyl electrophiles due to competitive β-hydride elimination.[5b] Although direct allylic C(sp^3)–H functionalization and oxidative Heck variants successfully bypass the need for halogenated starting materials, both pathways typically rely on stoichiometric quantities of harsh terminal oxidants to regenerate the active metal catalyst. Consequently, the resulting oxidative environment severely restricts the substrate scope by degrading sensitive or electron-rich nucleophiles.[10] Furthermore, both allylic and vinylic functionalization struggle to achieve high regio- and stereoselectivity when applied to electronically unbiased or sterically encumbered internal alkenes, and several attempts to install temporary directing groups ultimately erode the fundamental step- and atom-economy.[11] Recently, visible-light photocatalysis has offered a sustainable, selective, and mechanistically distinct platform for modern organic synthesis by enabling redox-controlled access to radical reactivity, owing to its ability to promote reactions under mild conditions.[12] By employing low-energy visible light, reactions can be conducted at ambient temperature, resulting in enhanced functional-group tolerance and reduced substrate decomposition. More importantly, the clear mechanistic distinction compared with transition-metal catalysis offers an opportunity to resolve any remaining issues related to substrate scope and selectivity.

When exposed to visible light, the photocatalyst produces reactive radical intermediates that can perform the allylic and vinylic C–H bond functionalization of simple alkenes *via* radical mechanisms (Scheme 1A). For example, the radicals generated by photocatalysis can activate allylic C(sp^3)–H bonds *via* hydrogen atom transfer (HAT) to form allylic radicals for subsequent reactions with various electrophiles, heteroatoms, or unsaturated partners (Scheme 1B). In addition, the direct oxidation of simple alkenes *via* single-electron transfer (SET) with an excited-state photocatalyst provides another route to access the corresponding allylic radical intermediate for allylic C(sp^3)–H functionalization (Scheme 1B). Alternatively, photogenerated radical intermediates can initiate radical addition/elimination pathways to provide various functionalized alkenes (Scheme 1B). Such differences in the mechanistic pro-

Juyoung Yang

Juyoung Yang was born in Busan, Republic of Korea, in 2003. She obtained her B.S. degree in Chemistry from Gyeongsang National University in 2026. In the same year, she joined the research group of Prof. Jungwon Kim at Gyeongsang National University as an M.S. student. Her research interests focus on multicomponent catalytic organic synthesis.

Jungwon Kim

Jungwon Kim was born in Suwon, Republic of Korea. He received his B.S. degree (2014) and Ph.D. (2020) from Seoul National University under the supervision of Prof. Soon Hyeok Hong. Following graduation, he pursued his research career as a postdoctoral researcher at the Max-Planck-Institut für Kohlenforschung (2020–2023) and the University of Münster (2024). Since September 2024, he has been an assistant professor at Gyeongsang National University. His research interests mainly focus on the development of sustainable catalytic strategies for organic synthesis.

This journal is © The Royal Society of Chemistry 2026

Open Access Article. Published on 18 May 2026. Downloaded on 5/26/2026 2:04:15 AM.
This article is licensed under a Creative Commons Attribution 3.0 Unported Licence.

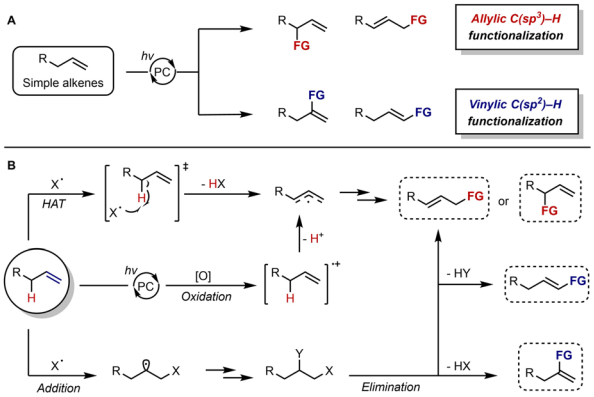

Scheme 1 Visible-light photoredox catalysis for allylic and vinylic C–H bond functionalization: Mechanistic consideration.

files of allylic and vinylic C–H bond functionalization are primarily derived from their distinct bond dissociation energies (BDEs). In general, allylic C(sp^3)–H bonds possess relatively lower BDEs (~89 kcal mol^{-1}),[13] whereas vinylic C(sp^2)–H bonds are significantly stronger (~111 kcal mol^{-1}),[13] rendering their activation considerably more challenging *via* HAT process. This fundamental disparity plays a crucial role in governing reaction pathways and selectivity in C–H bond functionalization processes. These mechanistic approaches, established by visible-light photocatalysis, provide a sustainable and versatile platform for allylic and vinylic C–H bond functionalization, thereby expanding the synthetic toolbox for late-stage modification and complex-molecule synthesis.

This review focuses on representative discoveries from the past decade concerning the direct allylic and vinylic C–H bond functionalization of simple alkenes *via* visible-light photocatalysis.[14,15] Although the utilization of activated alkenes, such as silyl enol ethers,[16] enamines,[17] and electron-deficient alkenes,[18] have been published, this review focuses on unactivated alkenes such as aliphatic alkenes and styrene derivatives.

2. Allylic C(sp^3)–H functionalization *via* direct oxidation of alkenes

Some alkenes are electron-rich substrates that can be easily oxidized, enabling excited-state photocatalysts to perform SET by removing one electron from the π-system, producing radical cation intermediates (Scheme 1B).[19] This oxidation markedly increases the acidity of the allylic proton, allowing facile deprotonation.[20] The generated allylic radical intermediates can then undergo further functionalization to produce substituted allylic compounds.

Wu *et al.* reported the allylic/benzylic alkylation of unactivated allylic/benzylic compounds **1** with methylene malononitriles **2** using Fukuzumi's catalyst (**3**) as a potent photooxidant (Scheme 2).[21] Owing to the strong oxidizing ability of this organophotocatalyst (E^{red*} = +2.18 V *vs.* SCE in MeCN),[22] allylic

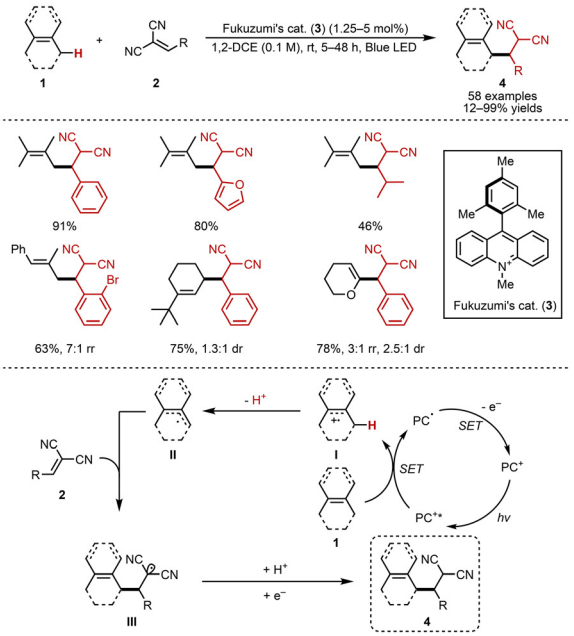

Scheme 2 Allylic C(sp^3)–H alkylation of alkenes with Michael acceptors.[21]

and benzylic radical intermediates are generated *via* single-electron oxidation followed by deprotonation. Tri-/tetra-substituted alkenes are suitable for photoredox processes because their relatively electron-rich nature enables their efficient oxidation by photocatalysts. Both acyclic and cyclic olefins were well tolerated under the reaction conditions. Regioselectivity was governed by both electronic and steric effects, with alkylation occurring preferentially at the least-hindered resonance site of the allylic radical, enabling controlled C–C bond formation. The proposed mechanism begins with SET-induced generation of the radical cation **I** from the alkene **1** *via* reductive quenching of the excited photocatalyst ($PC^{+}*$). Deprotonation of this radical cation **I** affords the allylic radical **II**, which undergoes nucleophilic addition to methylene malononitrile **2** at the less-hindered allylic position to produce the alkyl radical **III**. This electron-deficient radical intermediate **III** can accept single electron from the reduced form of the photocatalyst ($PC^{\bullet}$), and the subsequent protonation delivers the desired product **4**. Despite its significance, the methodology relies on electron-deficient olefins, thereby restricting the range of coupling partners. In addition, regioselectivity issues may arise in unsymmetrical substrates, resulting in the mixtures of constitutional isomers.

Glorius *et al.* developed a diastereoselective allylation of aldehydes using dual photoredox and chromium catalysis (Scheme 3).[23] They envisioned that the dual catalytic process would be initiated by photoexcitation of the Ir(III) complex [Ir(dF(CF_3)ppy)$_2$(dtbbpy)][PF_6] (**7**). Upon photoexcitation, the Ir(III) catalyst forms a highly oxidizing excited state ($E_{1/2}$(*Ir(III)/Ir(II)) = 1.21 V *vs.* SCE in MeCN)[24] that oxidizes the alkene **5**, generating an aryl radical cation **I**. Deprotonation yields allylic

Open Access Article. Published on 18 May 2026. Downloaded on 5/26/2026 2:04:15 AM.
This article is licensed under a Creative Commons Attribution 3.0 Unported Licence.

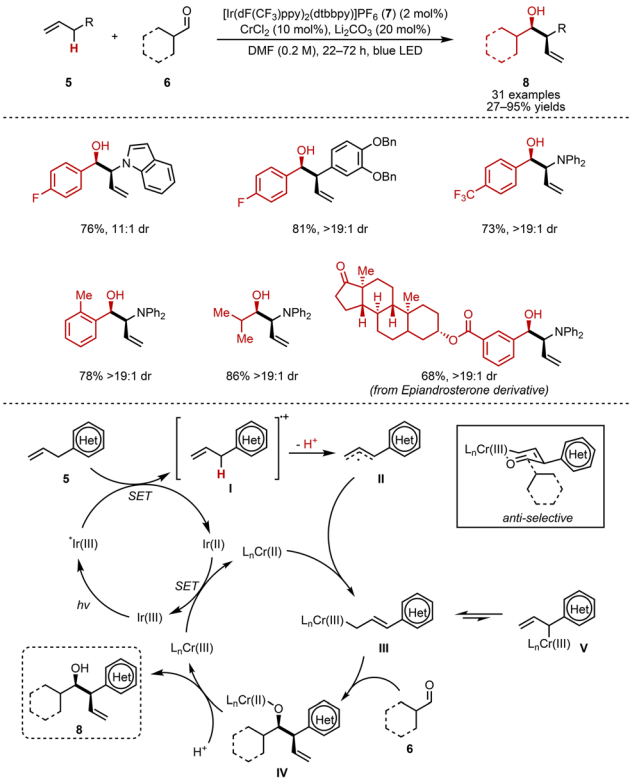

Scheme 3 Diastereoselective allylation of aldehydes with alkenes *via* dual photoredox and chromium catalysis. Reproduced with permission from ref. 23. Copyright 2018, American Chemical Society.

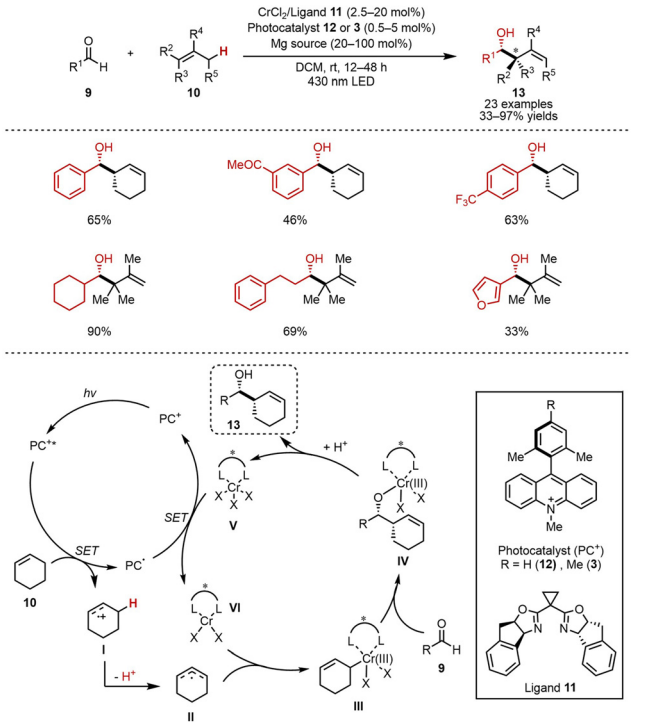

Scheme 4 Asymmetric allylation of aldehydes with alkenes *via* dual organophotoredox and chiral chromium catalysis.[25]

radical **II**, which is intercepted by low-valent Cr(II) to form Cr(III)-allyl species **III**. This reacts with an aldehyde **6** *via* a six-membered transition state, producing Cr(III)-alkoxide **IV**, which, after hydrolysis, affords the *anti*-selective homoallylic alcohol **8**. The catalytic cycles were closed by single-electron transfer between the reduced Ir(II) photocatalyst and the high-valent Cr(III) complex. This method enabled the selective allylation of both aliphatic and aromatic aldehydes, even when ketones and esters were present. The mild reaction conditions were compatible with a wide array of functional groups, as demonstrated by substrate scope studies and additive-based screening. However, this study was limited by its dependence on a relatively narrow substrate scope of alkenes, with optimal reactivity largely restricted to electronically activated systems, which may hinder broader applicability.

Kanai *et al.* reported an asymmetric allylation of aldehydes **9** using a hybrid catalytic system (Scheme 4).[25] In this process, nucleophilic chiral allylchromium(III) species **III** are generated *in situ* from hydrocarbon feedstock alkenes *via* allylic C(sp^3)–H bond activation. The mechanistic features closely parallel those described by Glorius (Scheme 3). In this case, the use of an acridinium-based photocatalyst **12** (PC^+) and an indane-BOX ligand **11** enables asymmetric C–C bond formation at the allylic position. The strong oxidizing power of acridinium photocatalysts allows broad compatibility with alkenes. Interestingly, $Mg(ClO_4)_2$ was crucial for achieving high reactivity and enantioselectivity, and the role of this additive was suggested to be the stabilization of the radical cation intermediate **I** by ClO_4^- *via* electrostatic interactions, as supported by transient-absorption spectrum measurements.

Yoon *et al.* developed a photoredox-based method for allylic sulfonamidation that proceed through a Cu(II)-mediated radical–polar crossover pathway (Scheme 5).[26] This approach enabled the preparation of a wide range of structurally diverse allylic amines. Upon light irradiation, triphenylpyrylium (**16**) is excited to a strongly oxidizing species that can undergo reductive quenching by alkene **14** through a SET process, generating radical cation **I**. The subsequent deprotonation of **I** occurs more rapidly than nucleophilic attack by the sulfonamide **15**, resulting in the formation of allylic radical **II**. The difference in these competing reaction rates accounts for the observed regioselectivity. In the final step, a Cu(II)-promoted radical–polar crossover occurs, enabling oxidative substitution to deliver the allylic C(sp^3)–H sulfonamidation product **17**.

Shu *et al.* developed a visible-light/cobalt dual catalytic strategy for the direct allylic C(sp^3)–H amination of alkenes with free amines, enabling efficient access to branched amines (Scheme 6).[27] The transformation proceeds with high regio- and chemoselectivity, selectively targeting the more sterically hindered position. This method offers a streamlined route to a wide range of primary, secondary, and tertiary aliphatic amines bearing diverse substitution patterns that are otherwise challenging to obtain. Initially, terminal alkene **18** undergoes visible-light-driven isomerization in the presence of a Co

This journal is © The Royal Society of Chemistry 2026

Open Access Article. Published on 18 May 2026. Downloaded on 5/26/2026 2:04:15 AM.
This article is licensed under a Creative Commons Attribution 3.0 Unported Licence.

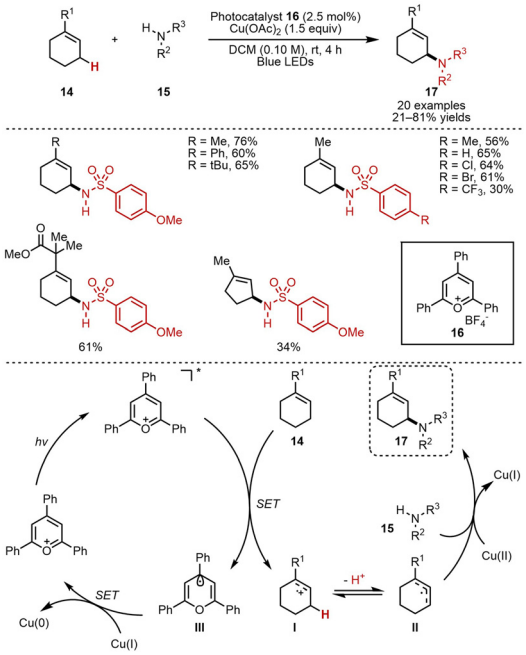

Scheme 5 Allylic C(sp^3)–H sulfonamidation of alkenes with sulfonamides *via* dual photoredox and copper catalysis. Reproduced with permission from ref. 26. Copyright 2023, American Chemical Society.

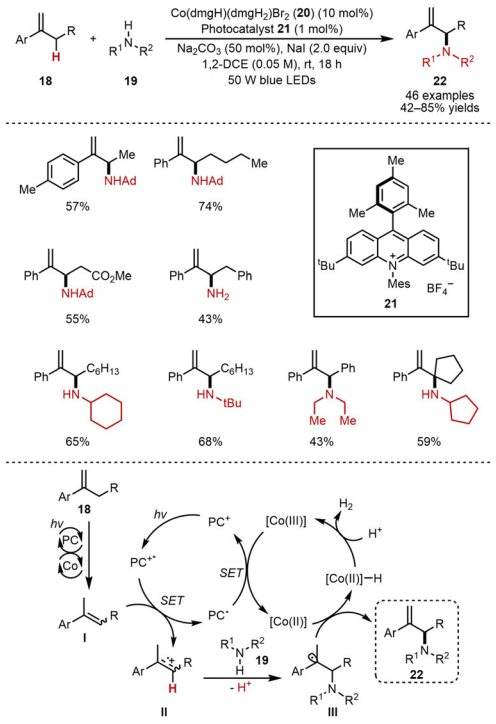

Scheme 6 Allylic C(sp^3)–H amination of alkenes with amines *via* dual photoredox and cobalt catalysis. Reproduced with permission from ref. 27. Copyright 2024, The American Association for the Advancement of Science.

catalyst to afford the corresponding internal alkene **I**. Upon irradiation, the photocatalyst **21** (PC^+) is promoted to its excited state (PC^+*), which is reductively quenched by **I** *via* SET, generating the reduced photocatalyst ($PC^•$) and radical cation intermediate **II**. This electrophilic intermediate **II** is subsequently trapped by nitrogen nucleophile **19**, forming a C–N bond and the carbon-centered radical **III**. Concurrently, the $PC^•$ species transfers an electron to the [Co(III)] catalyst, regenerating the ground-state photocatalyst **21** and producing [Co(II)], which then captures radical **III** and undergoes β-hydride elimination to furnish the desired product **22** in addition to a [Co(III)]–H intermediate. Protonation of the [Co(III)]–H species releases hydrogen gas (H_2) and restores the [Co(III)] catalyst, completing the catalytic cycle. Although an alternative pathway involving aminium radical cation formation cannot be entirely excluded, the slightly lower quenching efficiency of secondary amines compared to alkenes, together with the higher alkene-to-amine ratio (2.5 : 1) supports the reductive quenching cycle by alkene **18**.

3. Allylic C(sp^3)–H functionalization *via* hydrogen atom transfer (HAT)

Hydrogen atom transfer (HAT) is a key process in numerous chemical and biological reactions.[28] In particular, light-mediated HAT has been recognized as a potent instrument for the catalytic functionalization of aliphatic C(sp^3)–H bonds.[29] Taking advantage of the relatively weak bond-dissociation energy (BDE) of the allylic C(sp^3)–H bond (~89 kcal mol^{-1}),[13] HAT processes with several radical species have been utilized for allylic C(sp^3)–H bond functionalization (Scheme 1B).[30]

MacMillan *et al.* disclosed a dual photoredox and organocatalytic approach for achieving mild and efficient direct allylic C(sp^3)–H arylation (Scheme 7).[31] This C–C bond-forming transformation exhibits broad substrate compatibility, tolerating a wide variety of alkenes and electron-deficient arenes. Moreover, it has been successfully applied to the direct arylation of benzylic C–H bonds. The photoredox cycle begins with the light-induced excitation of the Ir photocatalyst **25** (Ir(III)), generating its excited state (*Ir(III)). This species engages in SET with 4-cyanopyridine, producing the corresponding radical anion **III** along with the oxidized form of the photocatalyst (Ir(IV)), which initiates the organocatalytic cycle by oxidizing the thiol catalyst **26** to form the thiyl radical **II**. Simultaneously, the ground-state photocatalyst **25** is regenerated. The resulting thiyl radical **II** then abstracts an allylic hydrogen atom from cyclohexene *via* the HAT process, affording the allylic radical **I**. Subsequent radical–radical coupling between intermediates, followed by cyanide elimination, leads to C–C bond formation and delivers the arylated product **27**, thereby completing both interconnected catalytic cycles.

Hong *et al.* reported a visible-light-driven photoredox strategy for the direct thiolation of allylic C(sp^3)–H bonds (Scheme 8).[32] In this approach, thiyl radical **I** produced *in situ* from disulfides **28** serve a dual role as HAT agents and coup-

Open Access Article. Published on 18 May 2026. Downloaded on 5/26/2026 2:04:15 AM.
This article is licensed under a Creative Commons Attribution 3.0 Unported Licence.

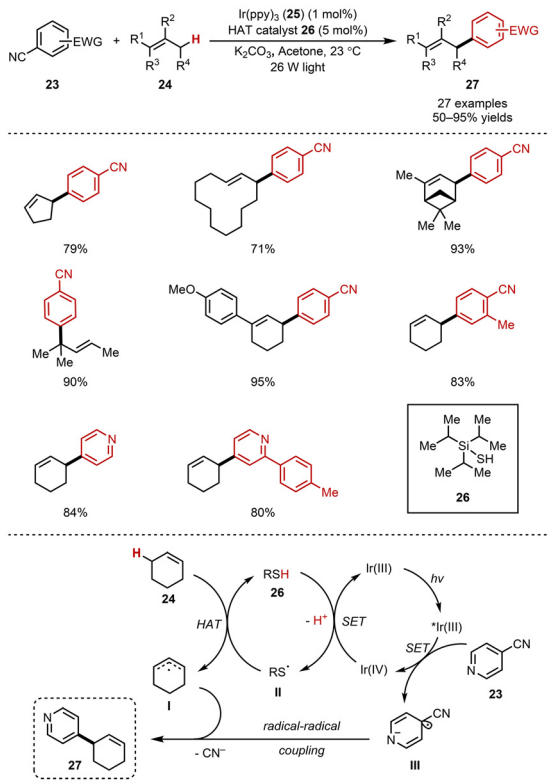

Scheme 7 Allylic C(sp^3)–H arylation with cyanoarenes. Reproduced with permission from ref. 31. Copyright 2015, Springer Nature.

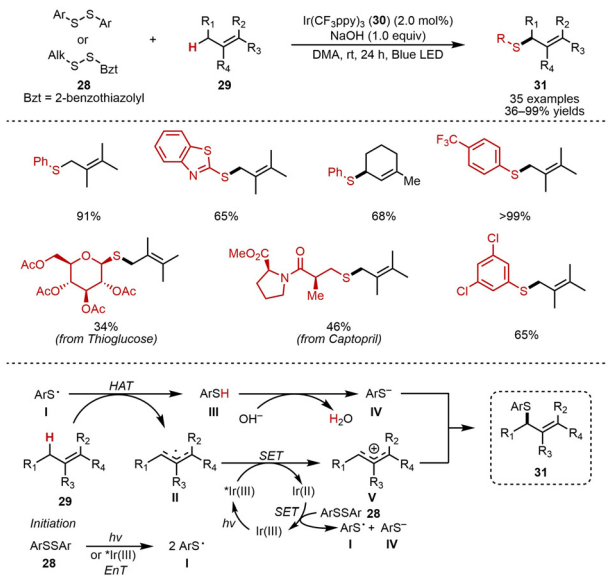

Scheme 8 Allylic C(sp^3)–H thiolation with disulfides. Reproduced with permission from ref. 32. Copyright 2020, American Chemical Society.

ling partners, enabling selective abstraction of an allylic hydrogen atom and subsequent C(sp^3)–S bond formation. This method provides an efficient route for producing allylic sulfides *via* controlled radical generation and interception under mild conditions. A plausible reaction mechanism begins with homolytic S–S bond cleavage, either *via* direct irradiation or energy transfer (EnT) from the photoexcited Ir(III)* species. The resulting thiyl radical **I** abstracts an allylic hydrogen atom from alkene **29** to generate the allylic radical **II**. Thiophenol **III** produced during HAT is rapidly deprotonated by hydroxide, suppressing back-hydrogen atom transfer during the undesired hydrothiolation pathway and rendering the desired HAT step effectively irreversible. The allylic radical **II** is subsequently oxidized by the photoexcited Ir(III)* species to an allylic cation **V**, which is trapped by thiolate **IV** to furnish the product **31**. Concurrently, the reduced Ir(II) photocatalyst is reoxidized to its ground-state Ir(III) form by diaryl disulfide **28**, regenerating both the thiyl radical **I** and thiolate **IV**. Although diverse, the substrate scope is biased toward electronically activated or pre-functionalized substrates, and the reaction efficiency can decrease with sterically hindered or unactivated partners.

Wu *et al.* developed an allylic C(sp^3)–H thiolation method achieved through cross-coupling between allylic and thiyl radicals (Scheme 9).[33] In this approach, the visible-light excitation of quantum dots (QDs)[34] as photocatalysts enables direct allylic C(sp^3)–H thiolation under exceptionally mild reaction conditions. Notably, this method eliminates the need for the pre-functionalization of either coupling partner, as well as any external oxidants or radical initiators, while generating H_2 as the only byproduct. Owing to their quantum confinement effects, diverse surface interactions, and strong, broad absorption across the visible spectrum, QDs provide a versatile platform for photocatalytic transformations. In particular, the CdSe QDs (**34**) activate allylic C(sp^3)–H and S–H bonds upon visible-light exposure, producing allylic and thiyl radicals **I** and **II**, respectively. The hydrogen atom abstracted from the allylic position can subsequently be reduced, forming H_2. Building

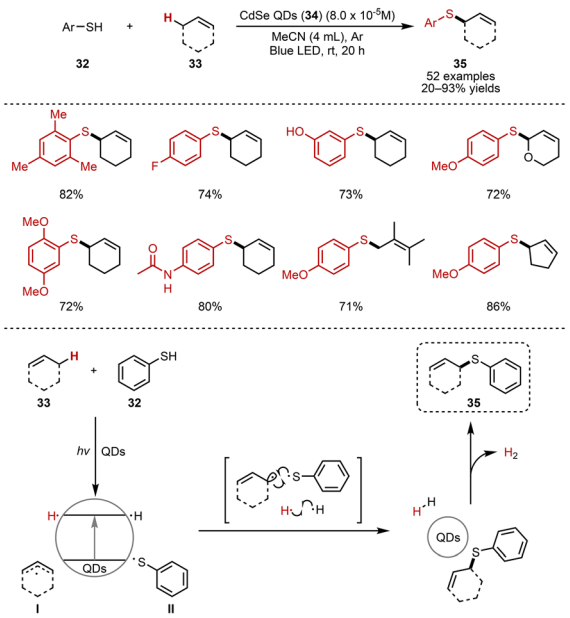

Scheme 9 Allylic C(sp^3)–H thiolation with thiols.[33]

This journal is © The Royal Society of Chemistry 2026

Open Access Article. Published on 18 May 2026. Downloaded on 5/26/2026 2:04:15 AM.
This article is licensed under a Creative Commons Attribution 3.0 Unported Licence.

on earlier reports of thiol activation on QD surfaces to generate thiyl radicals, the authors propose that these surface-bound thiyl radicals could trap allylic radical **I**, enabling radical–radical coupling to form allylic C–S bonds. This strategy enables the simultaneous activation of allylic C(sp^3)–H and thiol S–H bonds without requiring additional functional groups, external oxidants, or radical initiators. However, the reaction efficiency tends to decrease with sterically hindered or unactivated substrates.

Huang *et al.* reported an allylic C(sp^3)–H alkylation approach using imines that was initially designed *via* a radical–radical coupling mechanism, in which the allylic radical combines with a persistent radical anion formed through the SET reduction of the imine (Scheme 10).[35] However, the reduction potentials of imines (*e.g.*, $E_{1/2}$ = −1.91 *vs.* SCE in MeCN for *N*-benzylideneaniline) are significantly more negative than the redox potential of the reduced form of photocatalyst **7** ($E_{1/2}$[Ir(III)/Ir(II)] = −1.51 V), rendering the direct formation of a radical anion *via* SET to the imine thermodynamically unfavorable. Because several imines afford the desired products in good yields, the mechanism is proposed as the formation of a nitrogen-centered radical intermediate **III** by adding allylic radical **I** to imine **36**. This intermediate **III** is subsequently reduced by the Ir(II) species to deliver the final product **38**.

This dual photoredox/organocatalytic strategy can be further combined with other catalytic systems to expand the scope of coupling partners. Kanai *et al.* reported a catalytic strategy for the allylation of aldehydes using a broad range of alkenes based on a ternary hybrid catalytic system integrating photoredox, HAT, and chromium catalysis (Scheme 11).[36] This cooperative approach enables the direct utilization of readily available lower alkenes that cannot be easily oxidized *via* previously reported methods (Scheme 4), demonstrating wide substrate compatibility. Notably, this platform can be extended to enantioselective transformations *via* the incorporation of chiral ligands on a chromium catalyst. Upon photoexcitation, Nicewicz's acridinium photocatalyst **41** (E^{red}* = +2.09 V *vs.* SCE in MeCN)[22] oxidizes a HAT catalyst **42** *via* SET to generate a sulfur-centered radical **IV**, which selectively abstracts an allylic hydrogen atom from alkene **40** to form an allylic radical **I**. The resulting intermediate **I** is captured by a Cr(II) catalyst to form the allylchromium(III) intermediate **II**, which undergoes addition to aldehydes **39** through a chair-like transition state, delivering *anti*-homoallylic alcohols **43** after protonolysis. Subsequent single-electron reduction by the reduced acridinium catalyst (PC•) regenerates the active Cr(II) species, thus completing the catalytic cycle.

Glorius *et al.* expanded the area of ternary catalysis by incorporating nickel catalysts to achieve cross-coupling reactions between alkenes and aryl bromides (Scheme 12).[37] Nickel catalysis has successfully expanded the scope of arylation beyond electron-deficient cyanoarenes required for persistent radical precursors. A wide range of unactivated alkenes **44** can be functionalized with complex aryl bromides **45** in high yield and regioselectivity. The developed protocol can be applied to 1,5-hexadiene for the synthesis of several functionalized 1,4-dienes, which are important scaffolds for natural products. The HAT step was suggested to be the rate-limiting step, based on the observation of the primary KIE (4.0), and the DFT calculations suggested that a catalytic cycle including Ni(I)–Ni(III)–Ni(II)–Ni

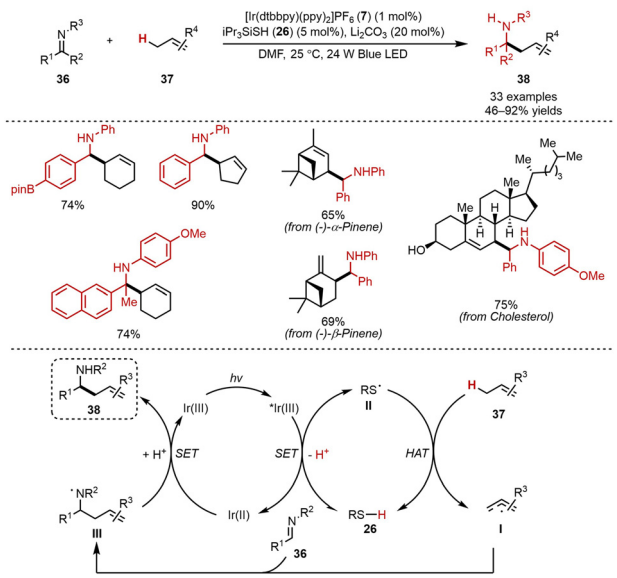

Scheme 10 Allylic C(sp^3)–H alkylation with imines.[35]

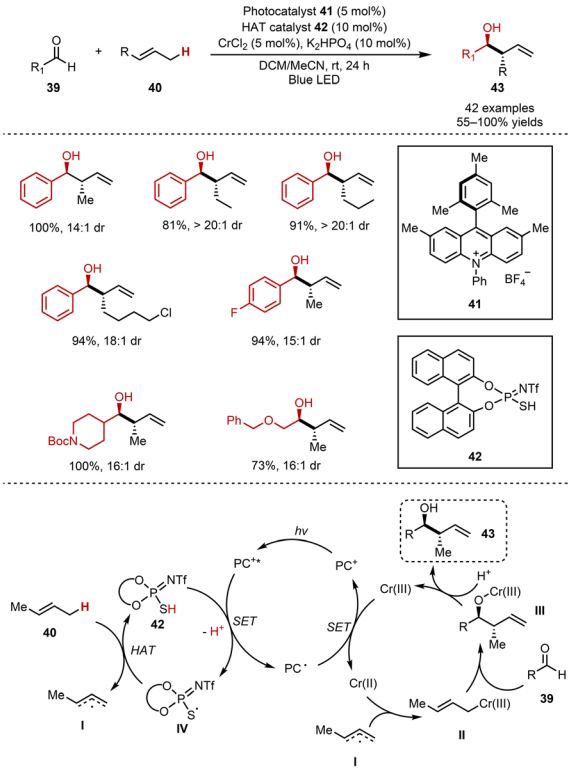

Scheme 11 Allylic C(sp^3)–H alkylation with aldehydes. Reproduced with permission from ref. 36. Copyright 2020, American Chemical Society.

Open Access Article. Published on 18 May 2026. Downloaded on 5/26/2026 2:04:15 AM.
This article is licensed under a Creative Commons Attribution 3.0 Unported Licence.

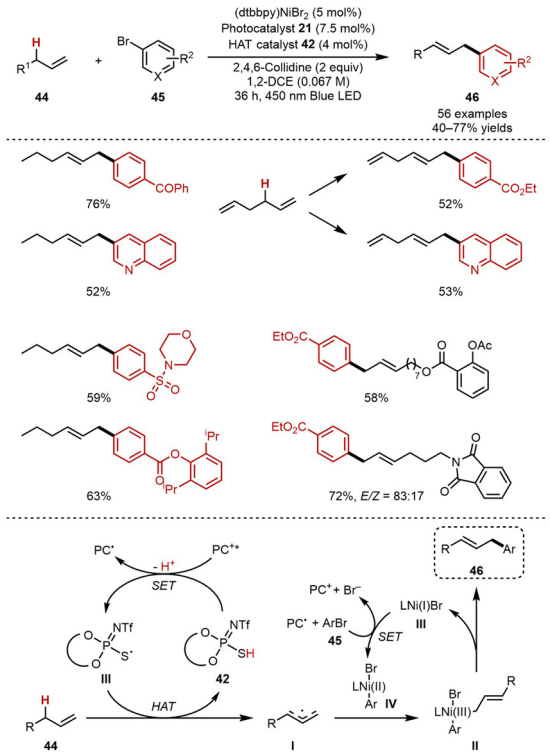

Scheme 12 Allylic C(sp^3)–H arylation with aryl bromides. Reproduced with permission from ref. 37. Copyright 2022, Springer Nature.

(III) for sequential oxidative addition, SET, radical capture, and reductive elimination is the most accessible pathway in the reaction.

Other organocatalysts, such as N-heterocyclic carbenes (NHC), can be used to further expand the scope of reactivity. Wang *et al.* developed a mild and operationally straightforward multicatalytic strategy to access β,γ-unsaturated ketones through allylic acylation of alkenes (Scheme 13).[38] This approach integrates NHC organocatalysis with HAT and photoredox catalysis, thereby enabling efficient cross-coupling between abundant carboxylic acids and simple olefins. The protocol delivers a broad range of β,γ-unsaturated ketones with high structural diversity while avoiding undesired olefin migration. In this system, the carboxylic acid is first activated *in situ* by *N*,*N*-carbonyldiimidazole (CDI) to generate an acylating species **47**, which reacts with an NHC catalyst **49** to form an acyl azolium intermediate **I**. Under visible-light irradiation, SET from the reduced photocatalyst (Ir(II)) converts this intermediate to the azolium radical anion **II**. In parallel, the oxidation of an *in situ*-generated thiolate (RS^-) produces a thiyl radical ($RS^•$), which selectively abstracts an allylic hydrogen atom from the alkene **48**, furnishing the nucleophilic allylic radical **III**. Radical–radical coupling between this allylic species **III** and the azolium radical anion **II** then delivers the desired β,γ-unsaturated ketone **50**. Although a reasonably wide substrate scope was demonstrated, diminished reactivity was observed with sterically hindered or electronically neutral alkenes. Issues related to

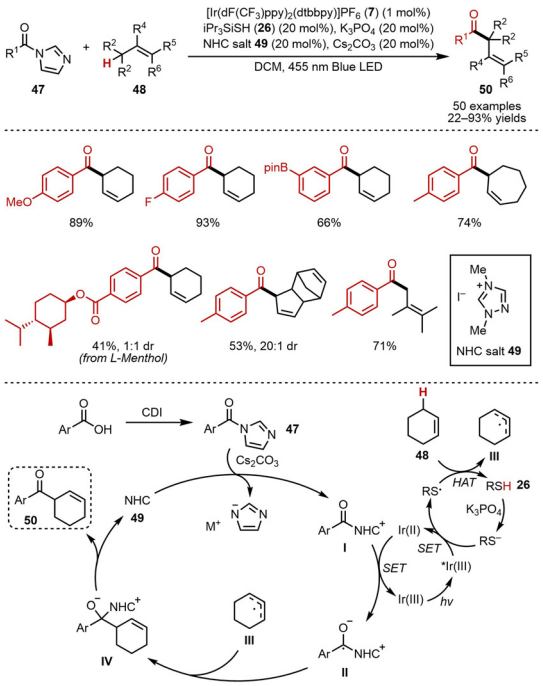

Scheme 13 Allylic C(sp^3)–H acylation.[38]

competing side reactions, such as radical recombination and undesired overfunctionalization, can compromise selectivity in more complex systems.

Melchiorre *et al.* described a radical-mediated organocatalytic approach that enabled the direct benzylation of allylic C(sp^3)–H bonds (Scheme 14).[39] The reaction was initially

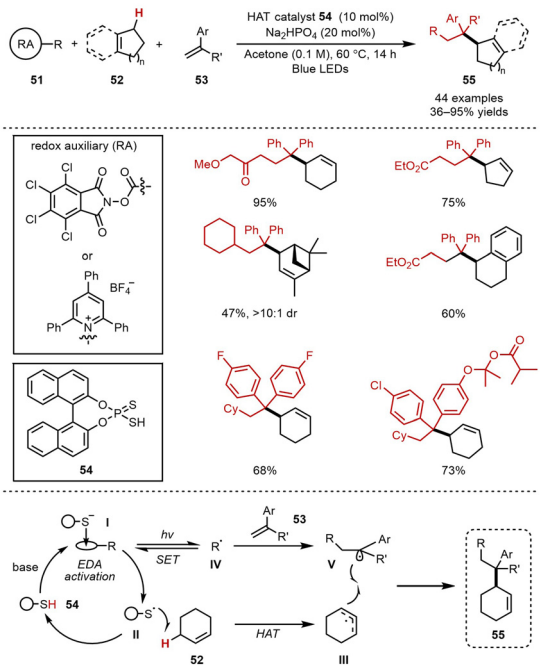

Scheme 14 Allylic C(sp^3)–H benzylation. Reproduced with permission from ref. 39. Copyright 2022, American Chemical Society.

This journal is © The Royal Society of Chemistry 2026

Open Access Article. Published on 18 May 2026. Downloaded on 5/26/2026 2:04:15 AM.
This article is licensed under a Creative Commons Attribution 3.0 Unported Licence.

designed for the radical–radical coupling of benzylic and allylic radicals that are generated *via* electron donor–acceptor (EDA) activation and SET. The diminished reactivity when the benzylic radical is replaced to a simple alkyl radical **IV** aligns with the proposed radical–radical coupling mechanism, which necessitates that the radical intermediate possesses sufficient kinetic persistence to effectively couple with the allylic radical **III**, consistent with the persistent radical effect. Guided by this consideration, the authors tried to extend the scope of the strategy by engaging the non-stabilized alkyl radical **IV**, which was generated through the catalytic EDA activation of suitable precursors, with the styrene derivative **53**. This approach resulted in the formation of benzylic radical **V**, whose enhanced persistence promoted efficient coupling with radical **III**, thereby enabling productive C–C bond formation. However, non-stabilized alkyl radicals fail to furnish the direct cross-coupling products, despite complete consumption of the corresponding radical precursors, thereby limiting this system.

Oxygen-centered radicals have also been utilized in the HAT process.[40] Because these radicals take advantage of the high BDE of the O–H bond (~105 kcal mol^{-1}),[13] they have been widely applied for the cleavage of unactivated C(sp^3)–H bonds. Nevertheless, several examples have been reported to achieve allylic C(sp^3)–H bond cleavages with oxygen-centered radicals as well.[41] For example, an enantioselective allylic C(sp^3)–H acyloxylation of internal alkenes was developed by Yu and co-workers (Scheme 15).[42] To overcome the conventional limitations of the Kharasch–Sosnovsky reaction, light energy was introduced to induce photoexcitation of the Cu(I) intermediate **II**, which can generate *tert*-butoxy radicals *via* oxidative quenching with *tert*-butyl peroxybenzoate **57**. This light irradiation enabled the allylic C(sp^3)–H bond cleavage *via* HAT and allylic radical generation under mild reaction conditions, which are suitable for asymmetric induction. The chiral Box ligand **58** provided the desired C–O bond formation product **59** with high enantio- and regioselectivity. The one-pot strategy for the *in situ* generation of peroxides, carboxylic acids, and DTBP significantly expanded the scope of the substrate, improving the utility of the developed reaction. The DFT calculation explained the origin of regioselectivity and enantioselectivity as the combinatorial effect of steric repulsion and C–H/π interaction in the most stable transition-state structure.

Halogen-centered radicals play key roles in the HAT process for both activated and unactivated C(sp^3)–H bonds.[43] In particular, Br radical can selectively cleave activated C(sp^3)–H bonds, achieving direct C(sp^3)–H bond functionalization under mild reaction conditions.[44] In 2018, Rueping *et al.* developed a novel protocol for direct allylic arylation/vinylation with aryl/vinyl bromides *via* metallaphotoredox catalysis (Scheme 16).[45] After the oxidative addition of aryl/vinyl bromides (**60**, **61**) to the L_nNi^0 catalyst, EnT by Fukuzumi's catalyst **3** can generate Br$^{\bullet}$ that can cleave allylic C(sp^3)–H bond of alkene **62** *via* a HAT process. Subsequent radical trapping by the Ni(II) intermediate **II** and reductive elimination results in C–C bond formation at the allylic position. Several functional groups were tolerated under the reaction conditions, and the transformation occurred at a less sterically hindered position.

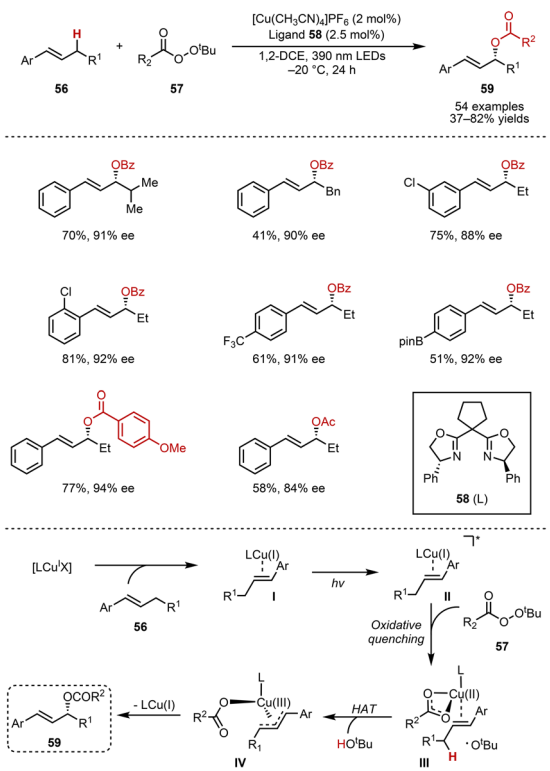

Scheme 15 Allylic C(sp^3)–H acyloxylation. Reproduced with permission from ref. 42. Copyright 2024, American Chemical Society.

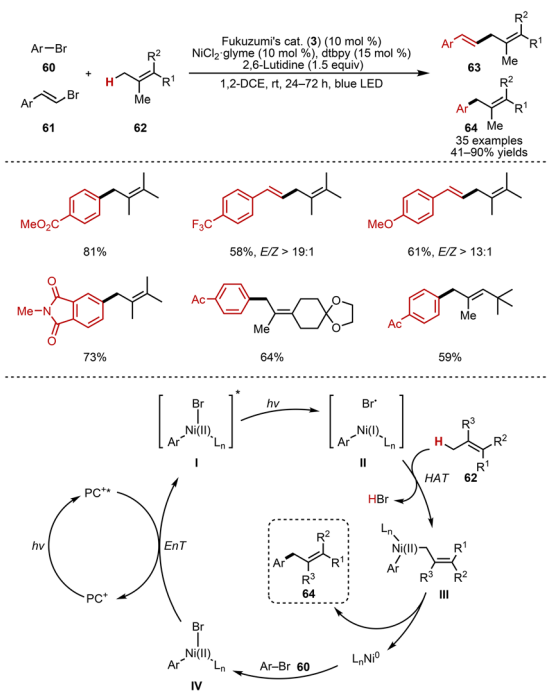

Scheme 16 Allylic C(sp^3)–H arylation/vinylation. Reproduced with permission from ref. 45. Copyright 2018, John Wiley & Sons.

Open Access Article. Published on 18 May 2026. Downloaded on 5/26/2026 2:04:15 AM.
This article is licensed under a Creative Commons Attribution 3.0 Unported Licence.

The utilization of a Br$^{\bullet}$ in allylic C(sp^3)–H bond functionalization was also demonstrated in direct allylic aerobic oxidation *via* organophotocatalysis using tetra-*n*-butylammonium bromide as a cocatalyst.[36]

Cai *et al.* reported a practical and efficient strategy for the direct oxidation of allylic C(sp^3)–H bonds mediated by visible-light photoredox catalysis (Scheme 17).[46] This transformation proceeds under mild, metal-free conditions at room temperature, utilizing molecular oxygen as the sole oxidant and delivering functionalized enones. Upon visible-light irradiation, Rose Bengal (**66**) is initially excited to its singlet state and then undergoes intersystem crossing to generate the corresponding triplet excited species. This triplet state transfers energy to ground-state molecular oxygen ($^3O_2$), producing highly reactive singlet oxygen ($^1O_2$, **I**), which subsequently reacts with the bromide ion to form a bromine radical. This bromine radical abstracts a hydrogen atom from the olefinic substrate **65**, thereby generating the key allylic radical **III**. Subsequently, **III** undergoes trapping by a superoxide radical anion **II**, followed by protonation and dehydration, ultimately furnishing the enone product **68**.

4. Allylic C(sp^3)–H functionalization *via* radical addition/elimination

Radical addition–elimination reactions constitute a powerful and mechanistically distinct strategy for C–C and C–heteroatom bond formation, enabling selective functionalization of the allylic positions of the substrate under mild conditions. A defining feature of these transformations is the sequential radical addition to a π-system, followed by elimination to regenerate unsaturation or expel a leaving group, thereby driving the reaction forward thermodynamically (Scheme 1B).

In 2020, Ritter and co-workers developed a novel method for direct allylic C(sp^3)–H amination of unactivated alkenes with iminothianthrenes (Scheme 18).[47] To synthesize alkyl allylamines from unactivated alkenes, a photoredox strategy was introduced to activate iminothianthrenes **70** *via* EnT. This activated intermediate **II** undergoes N–S bond cleavage to afford the nitrogen-centered radical **III** and thianthrene radical cation (TT$^{\bullet+}$) under acidic conditions. The generation of cationic intermediate **III** was proposed because no HAT reactivity was observed, likely due to the enhanced electrophilic character either through protonation or strong hydrogen-bonding interaction with hexafluoroisopropanol (HFIP). A regioselective addition of **III** to alkene **69** results in the formation of radical intermediate **IV**, which is trapped by the persistent TT$^{\bullet+}$ species to provide the di-functionalized intermediate **V**. Elimination of a proton and thianthrene (TT) occurs in the presence of the base to generate allylamine **71**. This protocol avoids the formation of aziridines by using an iminothianthrene species, which generates protonated amine radical species that are not involved in the intramolecular substitution after the radical addition. The reaction can be applied to both acyclic and cyclic alkenes, and several mechanistic studies,

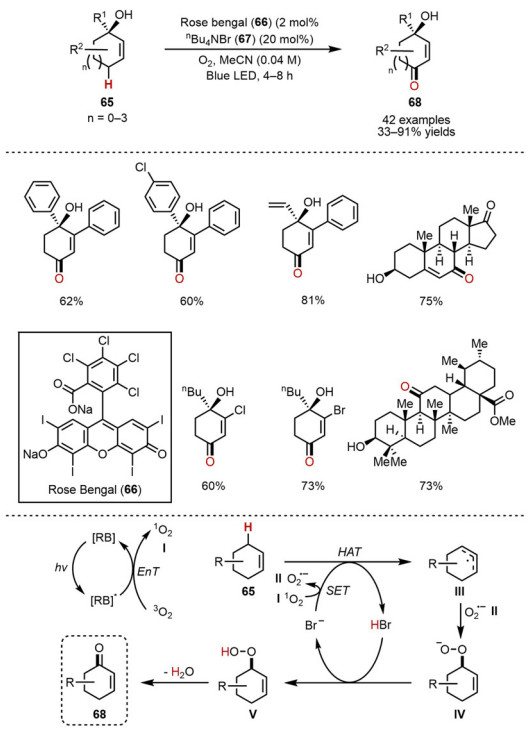

Scheme 17 Allylic C(sp^3)–H oxygenation.[46]

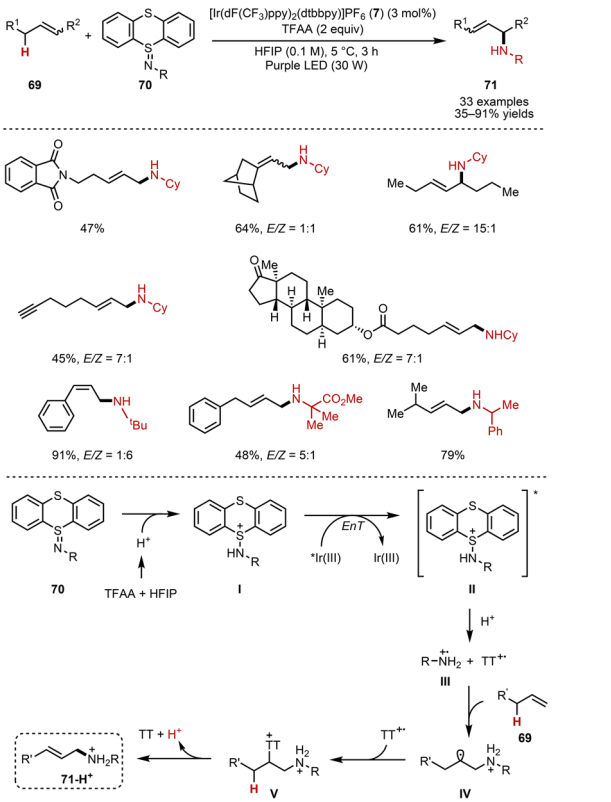

Scheme 18 Allylic C(sp^3)–H amination with iminothianthrenes.[47]

This journal is © The Royal Society of Chemistry 2026

Open Access Article. Published on 18 May 2026. Downloaded on 5/26/2026 2:04:15 AM.
This article is licensed under a Creative Commons Attribution 3.0 Unported Licence.

including Stern–Volmer quenching and radical trapping experiments, have suggested that the radical pathway operates in the reaction. However, the scope is limited for sterically hindered substrates, primarily due to slower radical addition and increased barriers for catalyst–substrate interaction.

Instead of the installation of a leaving group for the elimination, β-hydrogen elimination by a metal catalyst is the other option to provide the alkene product. Cobaloxime catalysis is a well-established strategy for several photochemical hydrogen elimination processes.[48] In 2022, Deng and co-workers developed a cooperative catalytic strategy integrating Brønsted base, cobalt, and photoredox catalysis facilitated by hydrogen-evolution-driven allylic C(sp^3)–H alkylation under mild, oxidant-free conditions (Scheme 19).[49] Upon visible-light excitation, the Ru(III) photocatalyst **74** engages in SET with the cobaloxime cocatalyst **75**, resulting in a high-valent Ru(IV) intermediate while simultaneously generating the catalytically active L_nCo(II) species. The strongly oxidizing Ru(IV) complex subsequently oxidizes the malonate anion **I** to produce a malonate-derived radical **II**. This carbon-centered radical **II** then undergoes addition to the alkene **73** to form a tertiary alkyl radical intermediate **III**. Product formation proceeds through cobalt-assisted β-hydrogen elimination from this intermediate **III**, delivering the desired coupled product **76** along with a L_nCo(III)–H species. Deuterium-labeling experiments indicate that the resulting L_nCo(III)–H intermediate can reversibly add to the alkene, accounting for the observed H/D exchange at the β-positions of the substrate or undergo protonation to release molecular hydrogen (H_2), thus completing the dehydrogenative catalytic cycle. Several alkenes can be utilized as sources for C–C bond formation with the activated methylene species, providing synthetically useful chemical synthons.

Amine organocatalysis induces the C–C bond formation between the α-position of carbonyl compounds and the allylic position,[50] and enantioselective transformation can be achieved by incorporating chiral amine organocatalysis.[51] In 2022, Luo and co-workers disclosed an enamine-enabled approach for controlling stereoselective planar cobalt metalloradical catalysis under visible-light photoredox conditions (Scheme 20).[52] In this cooperative system, chiral amine **81** operates in concert with cobaloxime catalyst **80** to promote radical addition, followed by the dehydrogenation of alkenes, ultimately delivering dehydrogenative allylic alkylation products with excellent enantioselectivity. The mechanism is proposed to proceed through a SET involving a Co(III)–Ir(IV)–enamine **I** assembly, which generates an α-imino radical intermediate **II** alongside a [Co(II)] metalloradical species. These two radical partners then act cooperatively in the addition to the alkene **78**, forming intermediate **III**, which subsequently undergoes light-driven dehydrogenation to furnish the allylated product **82** while producing a Co(III) hydride species ([Co(III)]–H). Hydrolytic release of the product restores the amine catalyst **81**, whereas reductive H_2 evolution regenerates the [Co(III)] species, thereby closing both catalytic cycles. Notably, the efficiency of the radical addition step is attributed to the transient formation of a radical–radical association, which is further reinforced by ion pairing between the protonated mor-

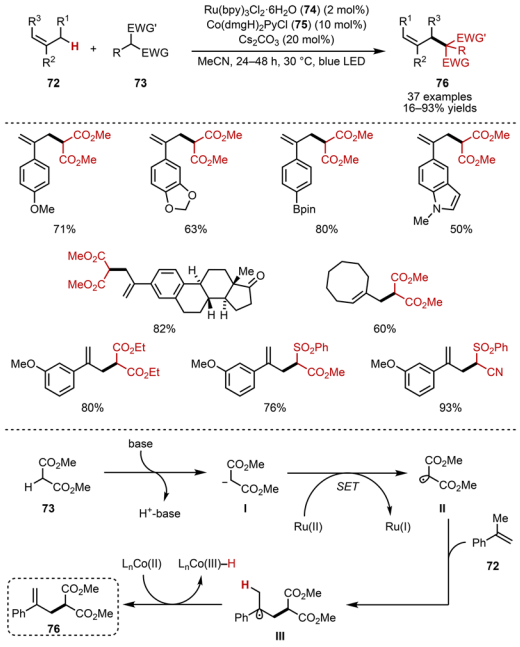

Scheme 19 Allylic C(sp^3)–H alkylation with malonate esters *via* dual Co/photocatalysis. Reproduced with permission from ref. 49. Copyright 2022, American Chemical Society.

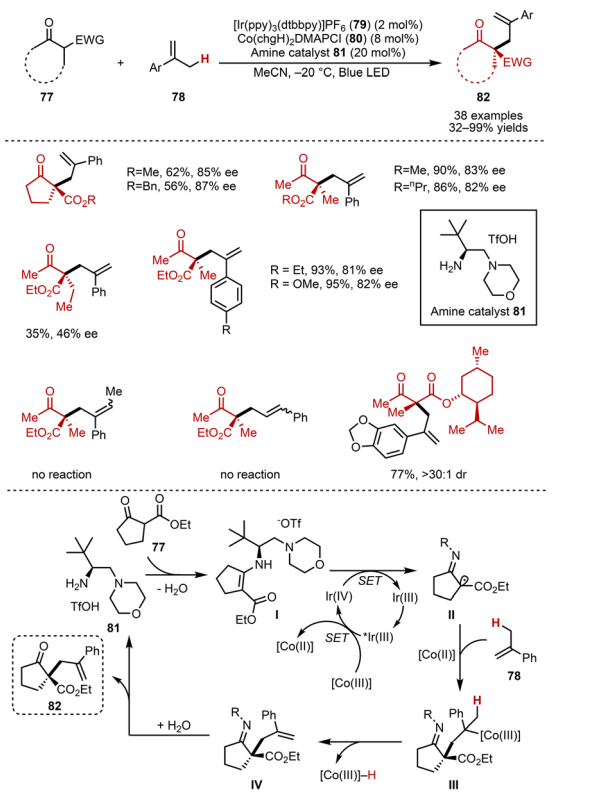

Scheme 20 Enantioselective allylic C(sp^3)–H alkylation.[52]

Open Access Article. Published on 18 May 2026. Downloaded on 5/26/2026 2:04:15 AM.
This article is licensed under a Creative Commons Attribution 3.0 Unported Licence.

pholine unit and the oxime anion. The developed protocol worked well for both simple and complex substrates; however, allylbenzenes and aliphatic alkenes were not reactive under the present reaction conditions.

This dual Co/photoredox strategy is also useful for C–heteroatom bond formation at allylic positions. Lei *et al.* presented an oxidant-free dehydrogenative sulfonylation of α-methyl styrene derivatives for the synthesis of allylic sulfones, utilizing Eosin Y (**85**) as a photosensitizer in conjunction with a cobaloxime catalyst **75** (Scheme 21).[53] Under visible-light irradiation, Eosin Y is promoted to its excited state (EY*, $E_{1/2}$ = +0.83 V *vs.* SCE), which undergoes reductive quenching by the sulfinate **I** generated *in situ via* deprotonation of the corresponding aryl sulfinic acid **83**. This process affords the Eosin Y radical anion ($EY^{\bullet-}$) in addition to a sulfonyl radical **II**. The subsequent addition of **II** to the α-methylstyrene derivatives **84** produces a carbon-centered radical **IV**, which is then oxidized by the Co(III) complex **V**, yielding the Co(II) species **VI** and a carbocation intermediate **VII** that furnishes the allylic sulfone **86** after deprotonation. Moreover, SET from $EY^{\bullet-}$ to the Co(II) species **VI** generates a Co(I) intermediate **VIII** and regenerates the ground-state EY, thereby completing the photoredox cycle. The resulting **VIII** can be protonated to evolve H_2; alternatively, a homolytic pathway involving the coupling of two Co(III)–H species to release H_2 cannot be excluded. Similar strategies have been applied for the use of sulfonyl hydrazine as a substrate[54] or C–P[55] bond formation at the allylic position in intermolecular coupling processes.

In 2022, Lei *et al.* also achieved the direct allylic amination of unactivated alkenes with simple secondary amines for the synthesis of tertiary aliphatic allylamines (Scheme 22).[56] The photoexcited iridium photocatalyst **7** (*Ir(III)) oxidizes the amine substrate **87** to generate the aminium radical cation **I**, which can engage in radical addition to electron-rich alkenes **88**. The generated carbon-centered radical **II** provides the desired allylamine **91** *via* HAT mediated by the [Co(II)] species. Extensive mechanistic studies, including DFT calculations, support the HAT process instead of β-hydrogen elimination, and the observed regioselectivity towards the terminal alkene formation was explained by the existence of hydrogen bonding between the protonated aminium moiety in the intermediate **II** and [Co(II)] species. A remarkably wide range of secondary cyclic and acyclic aliphatic amines could be allylated with simple alkenes with high regioselectivity, demonstrating the generality of the synthesis of functionalized tertiary allylamines. Similar reaction conditions can be utilized for intramolecular processes to obtain five-membered nitrogen cycles.[57]

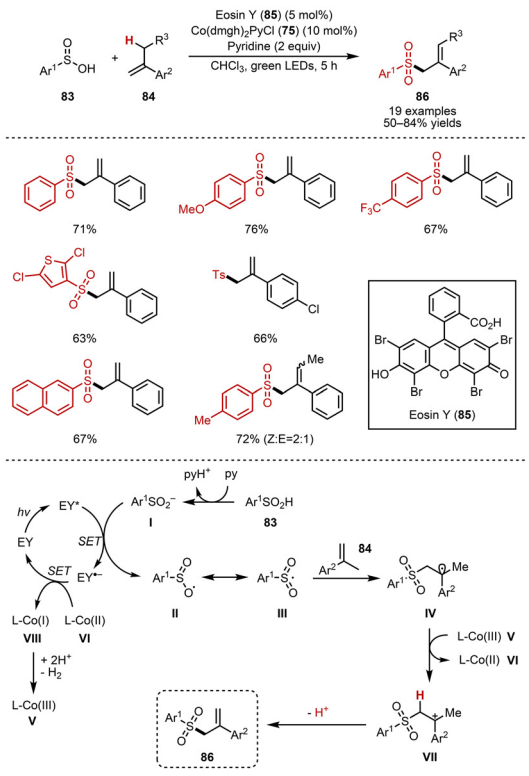

Scheme 21 Allylic C(sp^3)–H sulfonylation.[53]

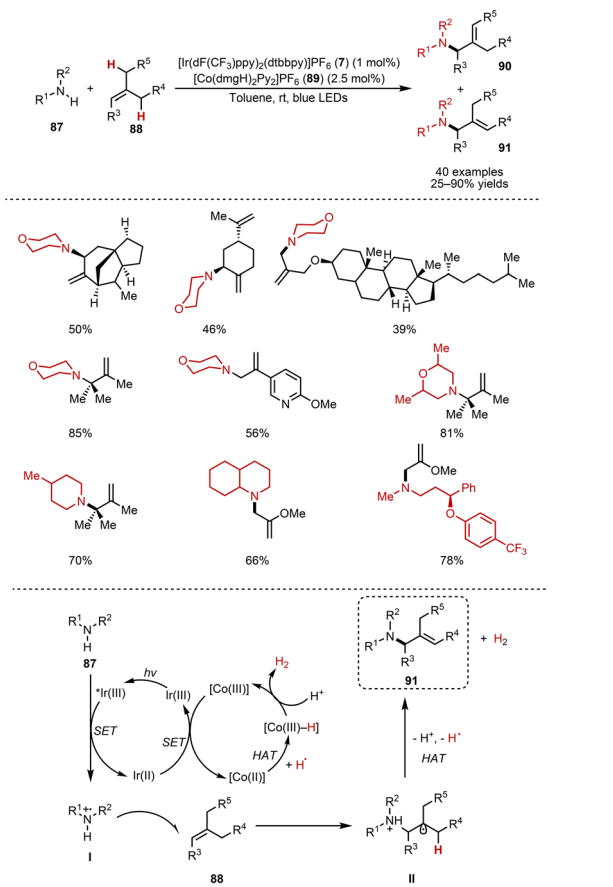

Scheme 22 Direct allylic C(sp^3)–H amination with secondary alkyl amines. Reproduced with permission from ref. 56. Copyright 2018, Springer Nature.

This journal is © The Royal Society of Chemistry 2026

Open Access Article. Published on 18 May 2026. Downloaded on 5/26/2026 2:04:15 AM.
This article is licensed under a Creative Commons Attribution 3.0 Unported Licence.

Instead of the cobaloxime species, copper catalysis has also been reported for β-hydrogen elimination in photoredox catalysis. In 2021, Hu *et al.* developed a direct allylic amidation of unactivated alkenes with Troc-protected carbamate **92** under dual Cu/photoredox catalysis conditions (Scheme 23).[58] A reasonable amount of alkene (3 equiv.) was sufficient to obtain synthetically useful yields of the allylamine products. Unfortunately, 1,1-disubstituted alkenes exhibit poor reactivity. The proposed mechanism starts with a SET between the photoexcited Ir(III)* catalyst and carbamate **92** to induce fragmentation towards the Troc-aminyl radical **I**, which can add to the alkene. The alkyl radical intermediate **II** is then trapped by the Cu(II)-OPiv species. β-hydrogen elimination with the Cu(III) intermediate **III** generates the allylamine **95** as a product, together with the regeneration of Cu(II)-OPiv *via* single-electron oxidation of Cu(I)–OPiv species. The origin of the regioselectivity was explained by the coordination of the Troc moiety to Cu(III) in the intermediate **III**, so that the pivalate ligand could access only H^1, leading to the formation of the allylamine **95**. This protocol is limited efficiency with sterically hindered and electronically neutral substrates due to sluggish radical addition and less favorable SET steps.

Bandini *et al.* described a novel route for the synthesis of allylic carboxylates from styrenes using visible-light photoredox catalysis (Scheme 24).[59] Instead of generating an oxygen-centered radical, direct oxidation of electron-rich alkene **96** was performed to induce the addition of a carboxylic acid **97** with anti-Markovnikov selectivity to generate the carbon-centered radical intermediate **II**. The *in situ*-generated [Co(II)] complex can then trap the radical intermediate **II**, and subsequent β-hydrogen elimination affords the desired product **98** and [Co(III)–H] species, which can be eventually reconverted to [Co(II)] *via* protonation. Both inter- and intramolecular coupling can be achieved under the developed reaction conditions, achieving direct allylic C(sp^3)–H oxygenation that usually requires transition-metal catalysis.[60]

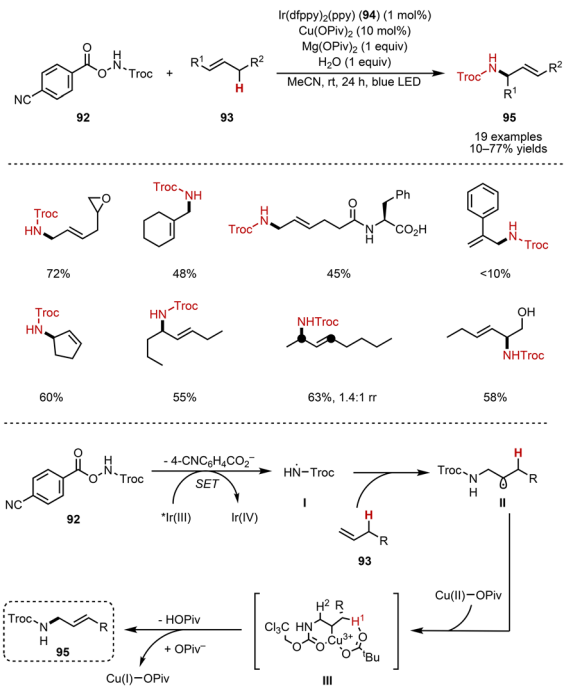

Scheme 23 Allylic C(sp^3)–H amination with Troc-protected carbamate ester.[58]

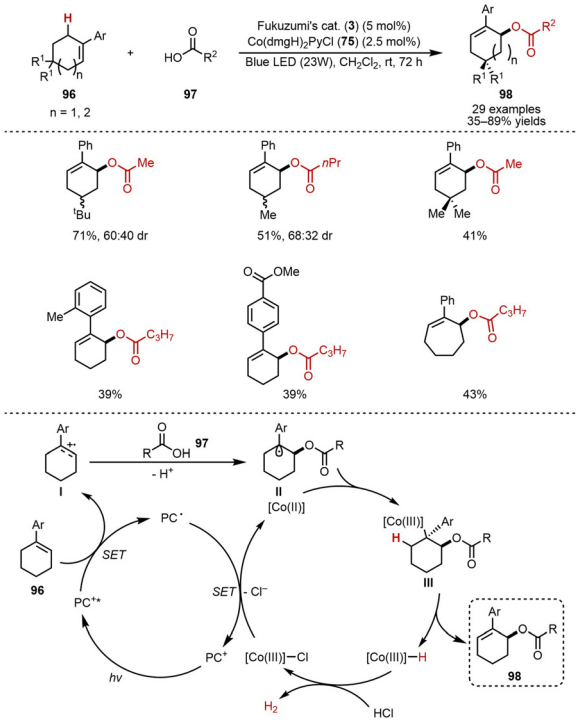

Scheme 24 Allylic C(sp^3)–H acyloxylation with carboxylic acids.[59]

5. Vinylic C(sp^2)–H functionalization *via* addition/elimination

Although the Heck reaction is a powerful method for constructing aryl-substituted alkenes, the branched-selective coupling of alkenes with pyridines remains challenging. Chu *et al.* developed a photoredox-catalyzed, sulfinate-assisted strategy for the branch-selective pyridylation of alkenes, which proceeded *via* a radical addition–coupling–elimination sequence using sodium sulfinates as recyclable radical sources and traceless leaving groups (Scheme 25).[61] A plausible mechanism involves an initial SET between the photoexcited *Ir(ppy)$_3$ (**25**, $E_{1/2}$ [*Ir(III)/Ir(IV)] = −1.73 V *vs.* SCE) and cyanopyridine **100**, which is feasible under appropriate conditions, yielding a pyridyl radical anion **I** along with an oxidizing Ir(IV) species. The resulting Ir(IV) intermediate ($E_{1/2}$ [Ir(IV)/Ir(III)] = +0.77 V *vs.* SCE) subsequently oxidizes methane sulfinate **II** ($E_{1/2}$ = +0.50 V *vs.* SCE), generating a sulfonyl radical **III** while regenerating the ground-state Ir(III) catalyst. This electrophilic radical **III** readily adds to the alkene **99** to form a nucleophilic benzylic radical intermediate **IV**, which then undergoes radical–radical

Open Access Article. Published on 18 May 2026. Downloaded on 5/26/2026 2:04:15 AM.
This article is licensed under a Creative Commons Attribution 3.0 Unported Licence.

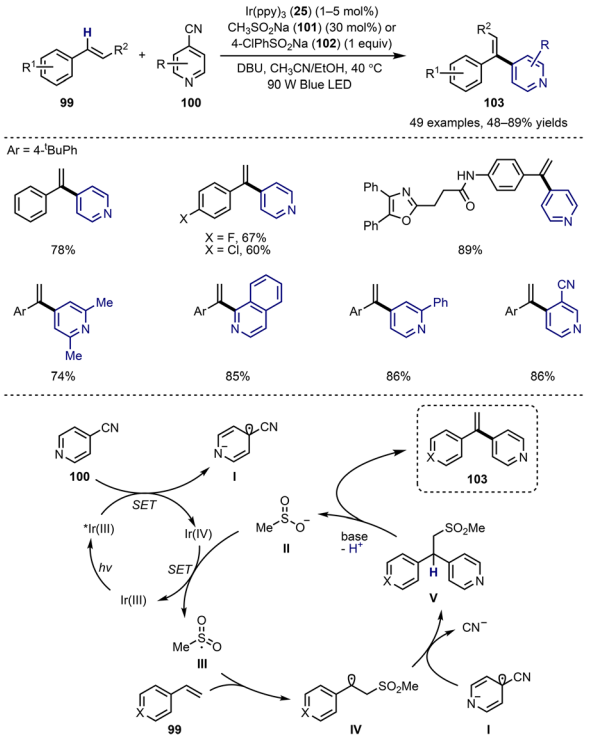

Scheme 25 Vinylic C(sp^2)–H pyridylation with cyanopyridines.[61]

coupling with the persistent pyridyl radical anion **I** to afford the β-sulfonyl pyridine intermediate **V**. Owing to the increased acidity of the benzylic proton and the good leaving group ability of the sulfone moiety, this intermediate **V** undergoes base-assisted E_1 elimination to furnish the branched alkenyl pyridine product **103** with the concurrent regeneration of sulfinate **II**, thereby sustaining the catalytic cycle.

Alkyl chlorides are challenging substrates in Pd-catalyzed Mizoroki–Heck reactions owing to the difficulty of C–Cl bond activation and competing β-hydride elimination. However, photoinduced Pd catalytic systems can overcome these limitations, enabling the efficient coupling of even tertiary alkyl chlorides under mild conditions with broad functional group tolerance, and enable the late-stage modification of complex bioactive molecules and the rapid construction of structurally intricate products. Hong *et al.* described a photoinduced Pd-catalyzed process in which the excitation of Pd(0) species **I** enables the reduction of alkyl chloride **105** to form an alkyl radical **III**, which then selectively adds to the β-position of styrene **104** to generate a Pd(I)/benzylic radical intermediate **V** (Scheme 26).[62] Continuous irradiation suppresses β-hydride elimination and facilitates Cl atom-mediated single-electron oxidation, producing a benzyl chloride **VI** while regenerating the Pd(0) catalyst **I**. Subsequent base-promoted elimination affords the Mizoroki–Heck coupling product **106**; however the possible involvement of photoexcited Pd species or higher-order Pd intermediates in direct single-electron oxidation pathways cannot be entirely ruled out.

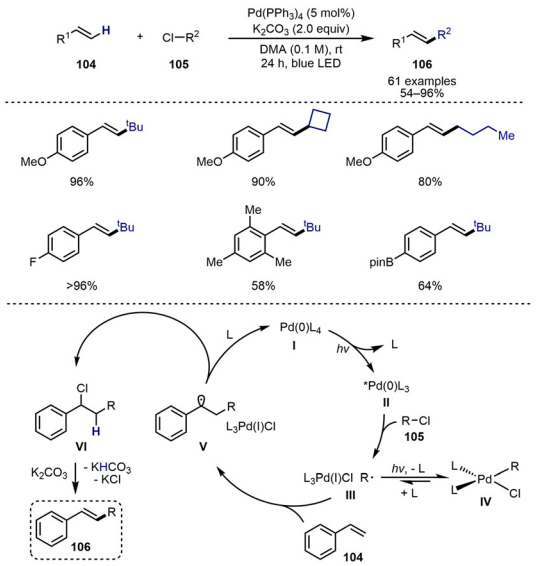

Scheme 26 Vinylic C(sp^2)–H alkylation with alkyl halides.[62]

If the regioselectivity is switched in the elimination step of the carbon-centered radical intermediate generated from the radical addition, the vinylic C(sp^2)–H functionalization of simple alkenes can be achieved. In particular, the direct vinylic C(sp^2)–H perfluoroalkylation of alkenes has been actively developed,[63] and certain studies have directed toward the utilization of organophotocatalysts.[64] For example, Bolm *et al.* demonstrated a visible-light-promoted atom transfer radical addition elimination process between terminal alkenes and perfluoroalkyl halides (Scheme 27).[65] Using Eosin Y (**85**) as a photoredox catalyst, perfluoroalkenes were obtained in good yields. Upon visible-light irradiation, excited Eosin Y under-

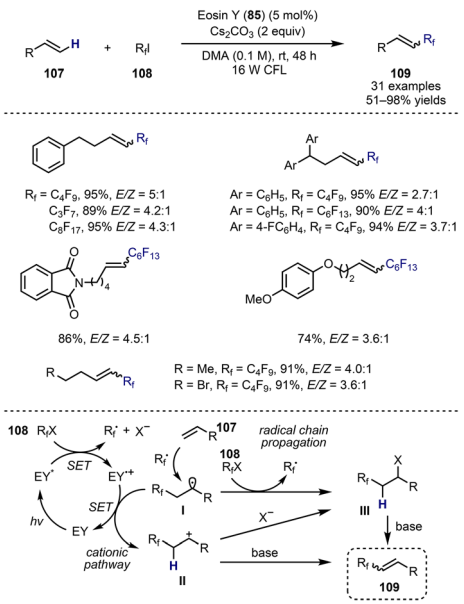

Scheme 27 Vinylic C(sp^2)–H perfluoroalkylation.[65]

This journal is © The Royal Society of Chemistry 2026

Open Access Article. Published on 18 May 2026. Downloaded on 5/26/2026 2:04:15 AM.
This article is licensed under a Creative Commons Attribution 3.0 Unported Licence.

goes oxidative quenching with the perfluoroalkyl halide **108**, producing a perfluoroalkyl radical (R_f) and halide anion. The resulting R_f radical adds to the alkene **107** to generate a carbon-centered radical intermediate **I**. This can proceed *via* two distinct pathways. In one route, the oxidation of **I** yields a carbocation **II**, which either directly or through an organohalide intermediate **III** furnishes the olefinic product **109** following base-mediated deprotonation. In the alternative pathway, intermediate **III** is formed through a radical chain propagation mechanism, ultimately leading to the same product outcome.

Zhu *et al.* developed a synthetic strategy towards the multisubstituted allylic and homoallylic azides (Scheme 28).[66] Depending on the structure of the starting allylic azides, the product can be either allylic azides *via* vinylic C(sp^2)–H alkylation or homoallylic azides *via* allylic C(sp^3)–H alkylation. After the generation of the carbon-centered radical intermediate **II** *via* the addition of the fluoroalkyl radical **I** to the allylic azide **110**, further SET oxidation by the oxidized photocatalyst Ir(IV) generates the carbocation intermediate **III**), leading to a radical-polar crossover. If the substituents on the allylic azide (R^1 or R^2) do not have any detachable protons, path **a** provides vinylic C(sp^2)–H alkylation products **112**. By contrast, the existence of detachable protons on either substituent of allyl azide leads to the formation of homoallyl azide product **113** *via* allylic C(sp^3)–H alkylation, according to path **b**. The use of bromodifluoroacetate (**111**) as an alkyl radical precursor proved to be efficient for radical addition to internal alkenes, affording tetrasubstituted alkenes **110** with high efficiency.

Sulfonyl fluorides are valuable compounds with broad applications, particularly in chemical biology and drug discovery owing to their unique biological properties. Consequently, efficient methods for their synthesis are in high demand. Liao *et al.* reported a novel photoredox strategy for the radical fluorosulfonylation of alkenes, in which FSO_2 radicals are generated under visible-light conditions (Scheme 29).[67] Photoexcitation of the Ir catalyst **7** enables a SET to chlorosulfonyl fluoride (**115**), producing the fluorosulfonyl radical **I**. This radical subsequently adds across the C–C double bond of the olefin **114**, yielding intermediate **II**. The resulting radical can further react with **115** to generate intermediate **III**, thereby propagating a chain mechanism, which is consistent with the detection of the chlorinated product in the radical clock experiment. Intermediate **II** then undergoes the elimination of HCl to afford the conjugated product **116**. Alternatively, a parallel redox pathway may also operate to some extent, involving the oxidation of **II** to **III** by the Ir(IV) species, followed by deprotonation.

In 2018, Wu *et al.* developed a photocatalytic decarboxylative Heck-type coupling of aliphatic carboxylic acids and terminal alkenes (Scheme 30).[68] The combination of Fukuzumi's catalyst (**3**) and a cobaloxime catalyst **119** enabled the decarboxylative coupling of various aliphatic carboxylic acids **117** and alkenes **118**. In addition to styrene species, vinyl boronates and silanes could also be utilized in the reaction. Further incorporation of acrylates promoted three-component reactions to produce highly functionalized alkene motifs. The mechanism of the reaction starts with SET from the carboxylic acid **117** to the highly oxidizing excited-state photocatalyst (PC^{+*}) to produce the alkyl radical **I** with the release of CO_2. The subsequent reaction of **I** with an alkene **118** generates a more stable benzylic radical intermediate **II**, which can be trapped by [Co(II)] to generate a [Co(III)] intermediate **III**. Subsequent β-hydrogen elimination through the homolytic

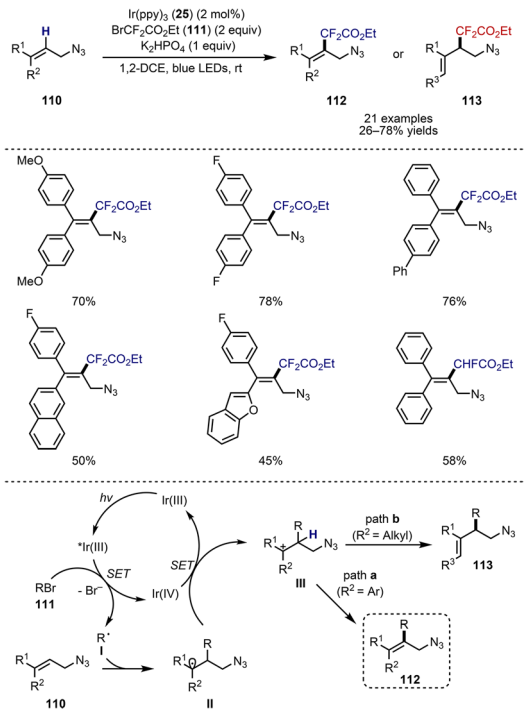

Scheme 28 Vinylic/allylic C–H alkylation with bromodifluoroacetate.[66]

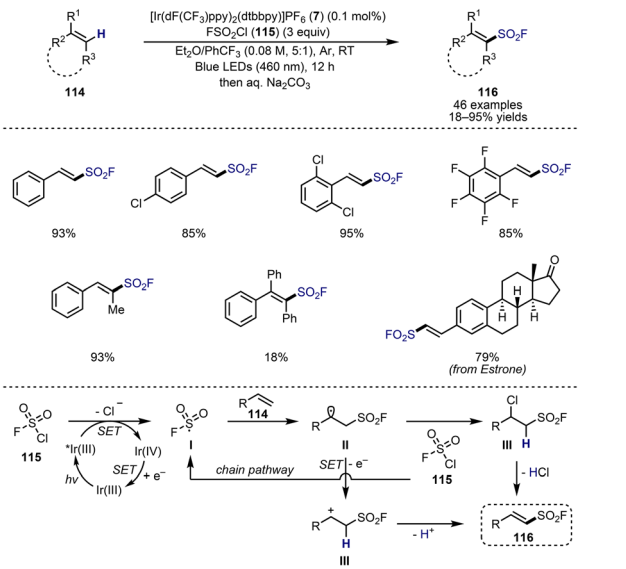

Scheme 29 Vinylic C(sp^2)–H fluorosulfonylation. Reproduced with permission from ref. 67. Copyright 2020, John Wiley and Sons.

Open Access Article. Published on 18 May 2026. Downloaded on 5/26/2026 2:04:15 AM.
This article is licensed under a Creative Commons Attribution 3.0 Unported Licence.

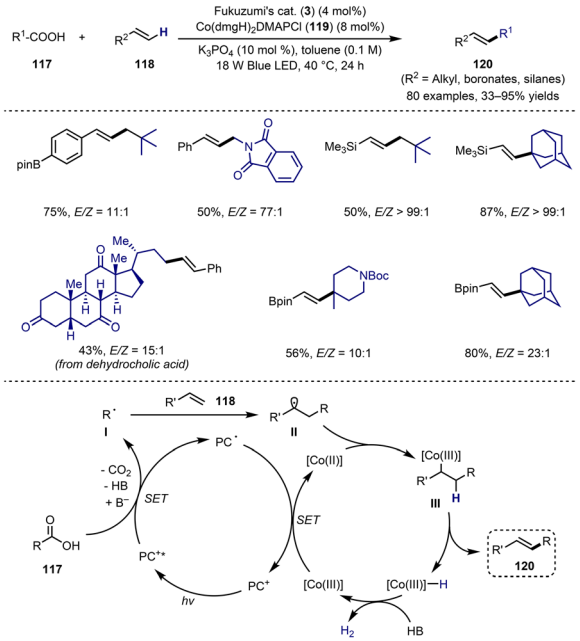

Scheme 30 Vinylic C(sp^2)–H alkylation with carboxylic acids. Reproduced with permission from ref. 68. Copyright 2018, American Chemical Society.

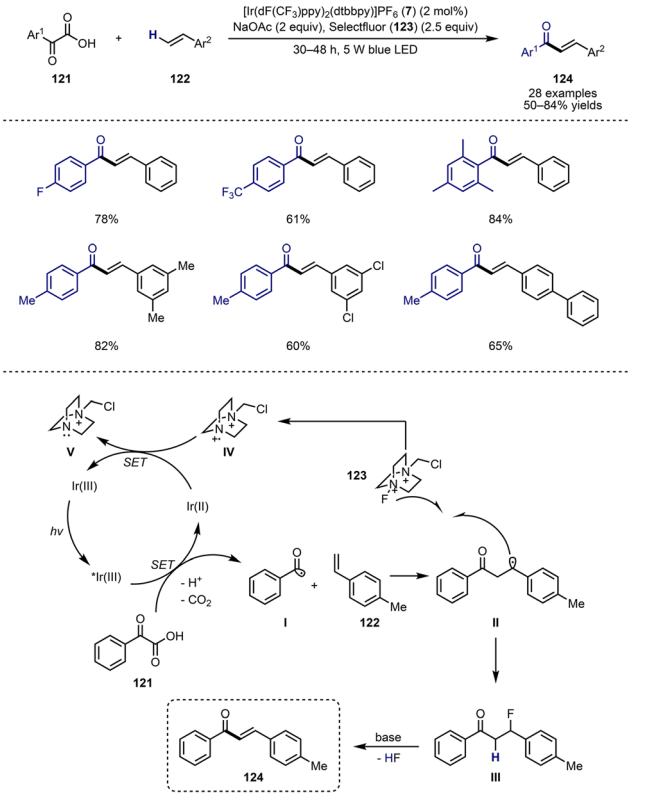

Scheme 31 Vinylic C(sp^2)–H acylation with α-keto acids.[70]

cleavage of the Co–C bond and β-hydrogen abstraction by [Co(II)] under blue-light irradiation produces the desired product **120**. An alternative mechanistic pathway, in which **I** is intercepted by a Co(II) species, followed by carbocobaltation to afford intermediate **III**, is not supported by DFT calculations because of the high energy barrier of the reaction pathway (46 kcal mol^{-1}).

The synthesis of α,β-unsaturated carbonyl compounds is an important strategy to obtain key building blocks.[69] Owing to their utility, several synthetic routes starting from readily available alkenes *via* photocatalytic regioselective acylation have been developed. For example, Zhu *et al.* synthesized substituted chalcones from α-keto acids and styrenes *via* sequential photocatalytic acylfluorination and HF elimination (Scheme 31).[70] The mechanism involves irradiation with an excitation of Ir catalyst **7** to its long-lived *Ir(III) state, which subsequently oxidizes the α-keto acid **121** through SET to generate Ir(II) and a carboxyl radical that rapidly undergoes decarboxylation to form an acyl radical **I.** The resulting **I** adds to styrene **122** to afford a benzylic radical **II**, which then undergoes fluorine atom transfer from Selectfluor (**123**) to construct the C–F bond, generating a Selectfluor radical cation **IV.** This species reoxidizes Ir(II) to Ir(III), thereby closing the catalytic cycle, while the acylfluorinated intermediate **III** undergoes base-promoted HF elimination to furnish the α,β-unsaturated ketone.

Later, aroylchlorination of alkenes *via* a 1,3-chlorine atom transfer was reported to deliver β-chloro ketones as latent enone intermediates by Ngai and co-workers (Scheme 32).[71] These masked enones **IV** can be smoothly converted into the

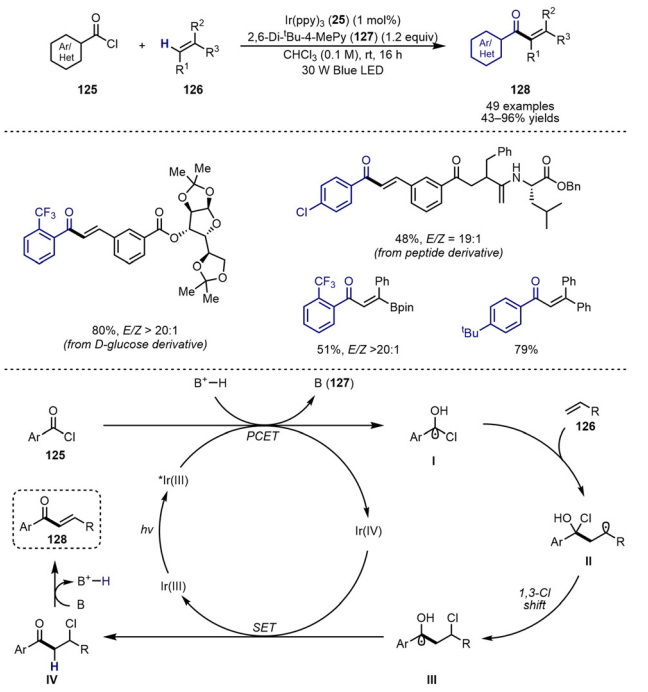

Scheme 32 Vinylic C(sp^2)–H acylation with acid chlorides.[71]

corresponding α,β-unsaturated ketones **128** upon workup, while simultaneously reducing competitive side reactions commonly associated with free enone products. Mechanistic

This journal is © The Royal Society of Chemistry 2026

Open Access Article. Published on 18 May 2026. Downloaded on 5/26/2026 2:04:15 AM.
This article is licensed under a Creative Commons Attribution 3.0 Unported Licence.

studies suggest that the reaction proceeds *via* a proton-coupled electron-transfer (PCET) mechanism, in which electrons and protons are transferred in a coordinated manner rather than in two completely independent steps. This process enables the generation of an α-chloro–α-hydroxy benzyl radical **I**, which subsequently undergoes radical addition and a 1,3-chlorine atom migration to drive product formation. In the presence of 2,6-di-*tert*-butyl-4-methylpyridinium salt (B–H$^+$), aroyl chloride **125** ($E_p \approx +1.02$ V *vs.* SCE) engages in a PCET with *Ir(III), resulting in the release of free base **127** (B) and formation of the α-chloro–α-hydroxy benzyl radical **I**. This nucleophilic radical subsequently undergoes addition to the alkene **126** substrate to generate the radical intermediate **II**, which then experiences a 1,3-chlorine atom migration to furnish the α-hydroxy radical **III**. Oxidation of **III** by Ir(IV) species, followed by deprotonation, regenerates the ground-state Ir(III) catalyst and yields the β-chloroketone **IV**. The final workup of this intermediate yields the corresponding enone **128**. The use of readily available acid chlorides **125** as an acyl source enables a wide range of acylation processes with densely functionalized styrene motifs to achieve late-stage functionalization.

Studer *et al.* developed a triple-relay catalysis integrating three distinct catalytic modes within a single process to synthesize α-branched enones (Scheme 33).[72] To switch the regioselectivity during acylation, a sulfinate radical was used for the radical addition step. Initially, the SET oxidation of aryl sulfinate **I** by an excited-state photocatalyst (*Ru(II)) generates an aryl sulfonyl radical **II**, and the subsequent addition of **II** to the alkene **129** affords the corresponding carbon-centered radical intermediate **III**. In a parallel pathway, the reaction of aroyl fluoride **130** with NHC catalyst **132** forms the acyl azolium species **V**, which undergoes SET reduction by the reduced photocatalyst (Ru(I)) to produce a ketyl-type radical **VI** while regenerating the ground-state photocatalyst (Ru(II)). Finally, the sequence of radical–radical cross-coupling between intermediates **III** and **VI**, NHC fragmentation, and elimination of sulfinate delivers the desired α-branched enone **133**. NHC organocatalysis efficiently converts acid fluoride into a redox-active acyl source, and the sulfinate cocatalyst acts as a facile leaving group to generate double bonds. The combined catalytic system works for various acid fluorides and styrenes, but the reaction with unactivated aliphatic alkenes was not successful.

Later in 2023, Ritter *et al.* reported the synthesis of α-branched enones from unactivated alkenes through regioselective chloroacylation with acyl chlorides (Scheme 34).[73] This strategy exploits the *in situ* generation of chlorine radicals from acyl chlorides under cooperative nickel/photoredox catalysis. Subsequent HCl elimination under basic conditions (DBU) furnishes α-branched enones **136** that are inaccessible through conventional acylation methods, which instead deliver the linear constitutional isomers. Several α-branched

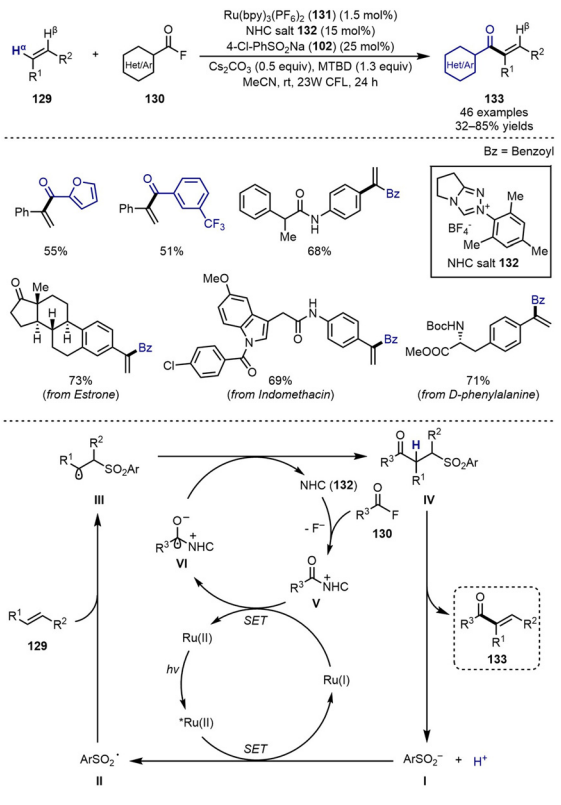

Scheme 33 Vinylic C(sp^2)–H acylation with acid fluorides *via* triple-relay catalysis.[72]

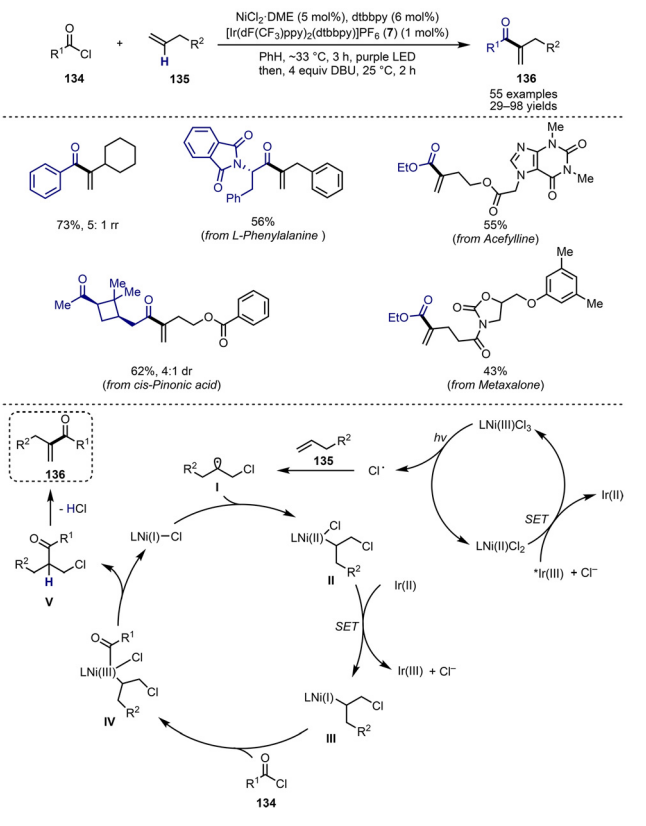

Scheme 34 Vinylic C(sp^2)–H acylation with acid chlorides *via* nickel/photoredox catalysis.[73]

Open Access Article. Published on 18 May 2026. Downloaded on 5/26/2026 2:04:15 AM.
This article is licensed under a Creative Commons Attribution 3.0 Unported Licence.

enones can be synthesized from either acid chlorides or carboxylic acids *via in situ* chlorination. In addition, the developed reaction conditions were also compatible with acid chloroformate, producing corresponding α-branched α,β-unsaturated esters in high selectivity. Based on the preliminary studies, a plausible mechanism was proposed as the generation of $Cl^{\bullet}$ by SET oxidation of $LNiCl_2$ (E°(Ni(III)/Ni(II)) = 0.72 V *vs.* SCE in MeCN) by the photoexcited Ir(III)* catalyst (E°(Ir(III)*/Ir(II)) = 1.21 V *vs.* SCE in MeCN). The direct oxidation of chloride is unlikely because of its significantly higher redox potential and the lack of reactivity observed in stoichiometric control experiments. The resulting $Cl^{\bullet}$ adds regioselectively to the terminal alkene to form the carbon-centered radical **I**, while the *in situ*-generated LNi(I)–Cl engages in coupling with the radical **I**. Subsequent oxidative addition with acid chloride **134** and reductive elimination furnishes the chloroacylated product **V**. By exploiting the high electrophilicity of $Cl^{\bullet}$, reactions with aliphatic unactivated alkenes can be achieved.

6. Conclusions

This review highlights recent advancements in the allylic and vinylic C–H functionalization of simple alkenes utilizing radical mechanisms *via* visible-light photocatalysis. With the diversification of catalytic systems for radical generation, various types of radical intermediates can react with alkenes. Direct single-electron oxidation induces the generation of allylic radical intermediates *via* facile deprotonation, and the utilization of the HAT process expands the substrate scope and reactivity towards alkenes that are difficult to be oxidized by the photocatalyst. The radical addition/elimination strategy provides another method for allylic C(sp^3)–H functionalization with precise control of regioselectivity, which further leads to formal vinylic C(sp^2)–H functionalization.

Despite the tremendous advances, significant challenges remain. First, the use of an excess amount of the alkene substrate limits the scope of volatiles or relatively small molecules. This limitation is due mainly to the side reactivity of the carbon-centered radical intermediates derived from alkenes, such as dimerization or polymerization. The incorporation of metal catalysts for the immediate trapping of radical intermediates partly reduces the amount of alkene, but most transformations still require a large excess of alkenes to suppress side reactivity. The use of internal or multisubstituted alkenes remains limited because of their innate steric hindrance and should be considered for future reaction development. In addition, more precise control of the reactive radical species is required to prevent other radical side reactions. More examples for the replacement of metal-based photocatalysts, such as Ru and Ir, with organic photocatalysts, such as cyanoarenes, will be required to achieve more sustainable synthetic strategies.[22,74] While allylic C(sp^3)–H functionalization has seen significant progress, the repertoire of visible-light-mediated vinylic C(sp^2)–H functionalizations remains underdeveloped. Broadening this field *via* the exploration of novel mechanistic strategies represents a crucial direction for future development. Finally, an in-depth study and development of reactions with high regioselectivity, stereoselectivity, and enantioselectivity are important for expanding the utility of visible-light photocatalysis for the direct functionalization of unactivated alkenes. In particular, achieving high levels of enantiocontrol in allylic C(sp^3)–H functionalization remains an essential goal that will undoubtedly expand the utility of visible-light photocatalysis in asymmetric late-stage modification and complex-molecule synthesis.[75] Overall, we anticipate that ongoing advances will broaden the use of such innovative strategies across diverse areas of organic synthesis.

Author contributions

The manuscript was written through contributions of all authors. All authors have given approval to the final version of the manuscript.

Conflicts of interest

The authors declare no competing financial interest.

Data availability

No primary research results, software or code have been included and no new data were generated or analysed as part of this review.

Acknowledgements

This work was supported by the research grant of the new professor of the Gyeongsang National University in 2024 (GNU-2024-240598). This work was also supported by the National Research Foundation of Korea grant (RS-2025-00513460) funded by the South Korean Government (MSIT).

References

1 (*a*) S. Patai, *The Chemistry of Alkenes*, Interscience Publishers, New York, 1964; (*b*) A. B. Flynn and W. W. Ogilvie, *Chem. Rev.*, 2007, **107**, 4698; (*c*) T. Tobrman and V. Hron, *Molecules*, 2025, **30**, 3370.
2 (*a*) Y. V. Kissin, Olefin Polymers, Introduction, in *Kirk-Othmer Encyclopedia of Chemical Technology*, John Wiley & Sons, Inc., 2005; (*b*) A. S. Elgharbawy and R. M. Ali, *Heliyon*, 2022, **8**, e09932; (*c*) X.-Y. Wang, Y. Gao and Y. Tang, *Prog. Polym. Sci.*, 2023, **143**, 101713.
3 I. P. Beletskaya and A. V. Cheprakov, *Chem. Rev.*, 2000, **100**, 3009.

 This journal is © The Royal Society of Chemistry 2026

Open Access Article. Published on 18 May 2026. Downloaded on 5/26/2026 2:04:15 AM. This article is licensed under a Creative Commons Attribution 3.0 Unported Licence.

4 (*a*) T. Mizoroki, K. Mori and A. Ozaki, *Bull. Chem. Soc. Jpn.*, 1971, **44**, 581; (*b*) R. F. Heck and J. P. Nolley Jr., *J. Org. Chem.*, 1972, **37**, 2320.

5 (*a*) M. Oestreich, *The Mizoroki-Heck Reaction*, John Wiley & Sons, New Jersey, 2009; (*b*) S. Jagtap, *Catalysts*, 2017, **7**, 267; (*c*) Y. Nakashima, G. Hirata, T. D. Sheppard and T. Nishikata, *Asian J. Org. Chem.*, 2020, **9**, 480; (*d*) D. Paul, S. Das, S. Saha, H. Sharma and R. K. Goswami, *Eur. J. Org. Chem.*, 2021, 2057.

6 (*a*) R. Wang, Y. Luan and M. Ye, *Chin. J. Chem.*, 2019, **37**, 720; (*b*) H.-M. Huang, P. Bellotti and F. Glorius, *Chem. Soc. Rev.*, 2020, **49**, 6186; (*c*) J. Grover, A. T. Sebastian, S. Maiti, A. C. Bissember and D. Maiti, *Chem. Soc. Rev.*, 2025, **54**, 2006.

7 (*a*) F. Liron, J. Oble, M. M. Lorion and G. Poli, *Eur. J. Org. Chem.*, 2014, 5863; (*b*) R. A. Fernandes and J. L. Nallasivam, *Org. Biomol. Chem.*, 2019, **17**, 8647; (*c*) P.-S. Wang and L.-Z. Gong, *Acc. Chem. Res.*, 2020, **53**, 2841; (*d*) P.-S. Wang and L.-Z. Gong, *Chin. J. Chem.*, 2023, **41**, 1841.

8 (*a*) T. A. F. Nelson, M. R. Hollerbach and S. B. Blakey, *Dalton Trans.*, 2020, **49**, 13928; (*b*) A. M. Kazerouni, Q. A. McKoy and S. B. Blakey, *Chem. Commun.*, 2020, **56**, 13287; (*c*) R. Manoharan and M. Jeganmohan, *Eur. J. Org. Chem.*, 2020, 7304.

9 (*a*) Z. Zhang, P. Chen and G. Liu, *Chem. Soc. Rev.*, 2022, **51**, 1640; (*b*) T. Aneeja, M. Neetha, C. M. A. Afsina and G. Anilkumar, *RSC Adv.*, 2020, **10**, 34429.

10 T. Dalton, T. Faber and F. Glorius, *ACS Cent. Sci.*, 2021, **7**, 245.

11 J. H. Docherty, T. M. Lister, G. Mcarthur, M. T. Findlay, P. Domingo-Legarda, J. Kenyon, S. Choudhary and I. Larrosa, *Chem. Rev.*, 2023, **123**, 7692.

12 (*a*) J. M. R. Narayanam and C. R. J. Stephenson, *Chem. Soc. Rev.*, 2011, **40**, 102; (*b*) C. K. Prier, D. A. Rankic and D. W. C. MacMillan, *Chem. Rev.*, 2013, **113**, 5322; (*c*) M. H. Shaw, J. Twilton and D. W. C. MacMillan, *J. Org. Chem.*, 2016, **81**, 6898; (*d*) N. A. Romero and D. A. Nicewicz, *Chem. Rev.*, 2016, **116**, 10075; (*e*) V. Srivastava, P. K. Singh and P. P. Singh, *J. Photochem. Photobiol., C*, 2022, **50**, 100488; (*f*) A. Y. Chan, I. B. Perry, N. B. Bissonnette, B. F. Buksh, G. A. Edwards, L. I. Frye, O. L. Garry, M. N. Lavagnino, B. X. Li, Y. Liang, E. Mao, A. Millet, J. V. Oakley, N. L. Reed, H. A. Sakai, C. P. Seath and D. W. C. MacMillan, *Chem. Rev.*, 2022, **122**, 1485; (*g*) N. Holmberg-Douglas and D. A. Nicewicz, *Chem. Rev.*, 2022, **122**, 1925.

13 S. J. Blanskyby and G. B. Ellison, *Acc. Chem. Res.*, 2003, **36**, 255.

14 For the selected reviews about the alkene functionalization *via* visible-light photocatalysis: (*a*) H. Yue, C. Zhu, L. Huang, A. Dewanji and M. Rueping, *Chem. Commun.*, 2022, **58**, 171; (*b*) G.-M. Cao, S.-S. Yan, L. Song, Y.-X. Jiang, T.-Y. Gao, Z. Chen, W. Zhang, J.-H. Ye and D.-G. Yu, *Chem. Soc. Rev.*, 2025, **54**, 6725.

15 For the selected reviews about the benzylic C(sp^3)–H bond functionalization: (*a*) M. Oliva, G. A. Coppola, E. V. Van der Eycken and U. K. Sharma, *Adv. Synth. Catal.*, 2021, **363**, 1810; (*b*) Y. Zhang, T. Zhang and S. Das, *Chem*, 2022, **8**, 3175; (*c*) F. Doraghi, S. Kermaninia, E. S. Ghalehsefid, B. Larijani and M. Mahdavi, *RSC Adv.*, 2025, **15**, 14691; (*d*) H. Zhu(s), Y. Wu, J. Mao, J. Xu, P. J. Walsh and H. Shi, *Chem. Soc. Rev.*, 2025, **54**, 2520.

16 (*a*) K. Ohmatsu, T. Nakashima, M. Sato and T. Ooi, *Nat. Commun.*, 2019, **10**, 2706; (*b*) T. Nakashima, H. Fujimori, K. Ohmatsu and T. Ooi, *Chem. – Eur. J.*, 2021, **27**, 9253.

17 (*a*) M. T. Pirnot, D. A. Rankic, D. B. C. Martin and D. W. C. MacMillan, *Science*, 2013, **339**, 1593; (*b*) F. R. Petronijević, M. Nappi and D. W. C. MacMillan, *J. Am. Chem. Soc.*, 2013, **135**, 18323; (*c*) J. A. Terrett, M. D. Clift and D. W. C. MacMillan, *J. Am. Chem. Soc.*, 2014, **136**, 6858; (*d*) E. R. Welin, A. A. Warkentin, J. C. Conrad and D. W. C. MacMillan, *Angew. Chem., Int. Ed.*, 2015, **54**, 9668.

18 (*a*) H. Xu, H. Zhang, Q.-X. Tong and J.-J. Zhong, *Org. Biomol. Chem.*, 2021, **19**, 8227; (*b*) K. Liu, D. Leifert and A. Studer, *Nat. Synth.*, 2022, **1**, 565; (*c*) J. Dong, Y. Hu, Y. Tang, F. Zhao, Y. Zhou and B. Fan, *Org. Chem. Front.*, 2024, **11**, 3562.

19 (*a*) M.-J. Luo, Q. Xiao and J.-H. Li, *Chem. Soc. Rev.*, 2022, **51**, 7206; (*b*) K. A. Margery and D. A. Nicewicz, *Acc. Chem. Res.*, 2016, **49**, 1997.

20 F. G. Bordwell, J.-P. Cheng and M. J. Bausch, *J. Am. Chem. Soc.*, 1988, **110**, 2872.

21 R. Zhou, H. Liu, H. Tao, X. Yua and J. Wu, *Chem. Sci.*, 2017, **8**, 4654.

22 A. Tlili and S. Lakhdar, *Angew. Chem., Int. Ed.*, 2021, **60**, 19526.

23 J. L. Schwarz, F. Schafers, T.-A. Adrian, L. Lückemeier and F. Glorius, *J. Am. Chem. Soc.*, 2018, **140**, 12705.

24 M. S. Lowry, J. I. Goldsmith, J. D. Slinker, R. Rohl, R. A. Pascal Jr., G. G. Malliaras and S. Bernhard, *Chem. Mater.*, 2005, **17**, 5712.

25 H. Mitsunuma, S. Tanabe, H. Fuse, K. Ohkubo and M. Kanai, *Chem. Sci.*, 2019, **10**, 3459.

26 G. A. Lutovsky, E. F. Plachinski, N. L. Reed and T. P. Yoon, *Org. Lett.*, 2023, **25**, 4750.

27 Y.-F. Ren, B.-H. Chen, X.-Y. Chen, H.-W. Du, Y.-L. Li and W. Shu, *Sci. Adv.*, 2024, **10**, eadn1272.

28 (*a*) P. R. Ortiz de Montellano, *Chem. Rev.*, 2010, **110**, 932; (*b*) J. M. Mayer, *Acc. Chem. Res.*, 2011, **44**, 36; (*c*) K. U. Ingold and D. A. Pratt, *Chem. Rev.*, 2014, **114**, 9022; (*d*) J. P. Klinman and A. R. Offenbacher, *Acc. Chem. Res.*, 2018, **51**, 1966; (*e*) J.-L. Tu and B. Huang, *RSC Sustain.*, 2024, **2**, 3222.

29 (*a*) S. Protti, M. Fagnoni and D. Ravelli, *ChemCatChem*, 2015, **7**, 1516; (*b*) H. Cao, X. Tang, H. Tang, Y. Yuan and J. Wu, *Chem Catal.*, 2021, **1**, 523; (*c*) L. Capaldo, D. Ravelli and M. Fagnoni, *Chem. Rev.*, 2022, **122**, 1875.

30 (*a*) H. Tanaka, K. Sakai, A. Kawamura, K. Oisaki and M. Kanai, *Chem. Commun.*, 2018, **54**, 3215; (*b*) S. Pradhan, G. Prakash and V. Gevorgyan, *J. Am. Chem. Soc.*, 2025, **147**, 43213.

Open Access Article. Published on 18 May 2026. Downloaded on 5/26/2026 2:04:15 AM. This article is licensed under a Creative Commons Attribution 3.0 Unported Licence.

31 J. D. Cuthbertson and D. W. C. MacMillan, *Nature*, 2015, **519**, 74.
32 J. Kim, B. Kang and S. H. Hong, *ACS Catal.*, 2020, **10**, 6013.
33 C. Huang, R.-N. Ci, J. Qiao, X.-Z. Wang, K. Feng, B. Chen, C.-H. Tung and L. Z. Wu, *Angew. Chem., Int. Ed.*, 2021, **60**, 11779.
34 (*a*) C. Huang, X.-B. Li, C.-H. Tung and L.-Z. Wu, *Chem. – Eur. J.*, 2018, **24**, 11530; (*b*) C. Huang, J. Qiao, R.-N. Ci, X.-Z. Wang, Y. Wang, J.-H. Wang, B. Chen, C.-H. Tung and L.-Z. Wu, *Chem*, 2021, **7**, 1244; (*c*) Y. Yuan, N. Jin, P. Saghy, L. Dube, H. Zhu and O. Chen, *J. Phys. Chem. Lett.*, 2021, **12**, 7180; (*d*) H.-L. Wu, M.-Y. Qi, Z.-R. Tang and Y.-J. Xu, *J. Mater. Chem. A*, 2023, **11**, 3262; (*e*) M. Navarro, J. Costa and F. L. N. Sousa, *ChemCatChem*, 2024, **16**, e202301740.
35 J. Jia, R. Kancherla, M. Rueping and L. Huang, *Chem. Sci.*, 2020, **11**, 4954.
36 S. Tanabe, H. Mitsunuma and M. Kanai, *J. Am. Chem. Soc.*, 2020, **142**, 12374.
37 H.-M. Huang, P. Bellotti, P.-P. Chen, K. N. Houk and F. Glorius, *Nat. Synth.*, 2022, **1**, 59.
38 X. Wang, R. Yang, B. Zhu, Y. Liu, H. Song, J. Dong and Q. Wang, *Nat. Commun.*, 2023, **14**, 2951.
39 E. L. Saux, M. Zanini and P. Melchiorre, *J. Am. Chem. Soc.*, 2022, **144**, 1113.
40 (*a*) L. Chang, Q. An, L. Duan, K. Feng and Z. Zuo, *Chem. Rev.*, 2021, **122**, 2429; (*b*) P. P. Singh, S. Sinha, P. Gahtori, S. Tivari and V. Srivastava, *Org. Biomol. Chem.*, 2024, **22**, 2523; (*c*) L. Müller, J. Poll, P. Nuernberger, I. Ghosh and B. König, *Chem. – Eur. J.*, 2025, **31**, e202404707.
41 N. Ishida, Y. Masuda, S. Uemoto and M. Murakami, *Chem. – Eur. J.*, 2016, **22**, 6524–6527; Y. Li, M. Lei and L. Gong, *Nat. Catal.*, 2019, **2**, 1016.
42 S. Tang, H. Xu, Y. Dang and S. Yu, *J. Am. Chem. Soc.*, 2024, **146**, 27196.
43 S. Bonciolini, T. Noël and L. Capaldo, *Eur. J. Org. Chem.*, 2022, e202200417.
44 B. Saxena, R. I. Patel and A. Sharma, *RSC Sustain.*, 2024, **2**, 2169.
45 L. Huang and M. Rueping, *Angew. Chem., Int. Ed.*, 2018, **57**, 10333.
46 C. Liu, H. Liu, X. Zheng, S. Chen, Q. Lai, C. Zheng, M. Huang, K. Cai, Z. Cai and S. Cai, *ACS Catal.*, 2022, **12**, 1375.
47 Q. Cheng, J. Chen, S. Lin and T. Ritter, *J. Am. Chem. Soc.*, 2020, **142**, 17287.
48 (*a*) M. Kojima and S. Matsunaga, *Trends Chem.*, 2020, **2**, 410; (*b*) P. Dam, K. Zuo, L. M. Azofra and O. El-Sepelgy, *Angew. Chem., Int. Ed.*, 2024, **63**, e202405775; (*c*) A. Mandal, M. Lim, L. Zhang, K.-W. Huang and S. U. Dighe, *ACS Catal.*, 2025, **15**, 9976.
49 M.-Y. Dong, C.-Y. Han, D.-S. Li, Y. Hong, F. Liu and H.-P. Deng, *ACS Catal.*, 2022, **12**, 9533.
50 J.-L. Liu, J.-L. Tu and F. Liu, *Org. Lett.*, 2020, **22**, 7369.
51 (*a*) C. Prentice, J. Morrisson, A. D. Smith and E. Zysman-Colman, *Beilstein J. Org. Chem.*, 2020, **16**, 2363; (*b*) W. Yao, E. A. Bazan-Bergamino and M.-Y. Ngai, *ChemCatChem*, 2022, **14**, e202101292; (*c*) C. D.-T. Nielsen, J. D. Linfoot, A. F. Williams and A. C. Spivey, *Org. Biomol. Chem.*, 2022, **20**, 2764.
52 Z. Jia, L. Zhang and S. Luo, *J. Am. Chem. Soc.*, 2022, **144**, 10705.
53 G. Zhang, L. Zhang, H. Yi, Y. Luo, X. Qi, C.-H. Tung, L.-Z. Wu and A. Lei, *Chem. Commun.*, 2016, **52**, 10407.
54 H. Xu, H. Zhang, Q.-X. Tong and J.-J. Zhong, *Org. Biomol. Chem.*, 2021, **19**, 8227.
55 A. Zhang, M.-M. Li, L. Guo, H. Yang, J. Guo, D. Xu and W. Ding, *Org. Chem. Front.*, 2025, **12**, 148.
56 S. Wang, Y. Gao, Z. Liu, D. Ren, H. Sun, L. Niu, D. Yang, D. Zhang, X. Liang, R. Shi, X. Qi and A. Lei, *Nat. Catal.*, 2022, **5**, 642.
57 W.-L. Yu, Z.-G. Ren, W. Ma, H. Zheng, W. Wu and P.-F. Xu, *Green Chem.*, 2022, **24**, 6131.
58 X. Yi and X. Hu, *Chem. Sci.*, 2021, **12**, 1901.
59 Y. Liu, S. Battaglioli, L. Lombardi, A. Menichetti, G. Valenti, M. Montalti and M. Bandini, *Org. Lett.*, 2021, **23**, 4441.
60 M. S. Chen and M. C. White, *J. Am. Chem. Soc.*, 2004, **126**(5), 1346; M. S. Chen, P. Narayanasamy, N. A. Labenz and M. C. White, *J. Am. Chem. Soc.*, 2005, **127**, 6970; A. N. Campbell, P. B. White, I. A. Guzei and S. S. Stahl, *J. Am. Chem. Soc.*, 2010, **132**, 15116; C. V. Kozack, J. A. Sowin, J. N. Jaworski, A. V. Iosub and S. S. Stahl, *ChemSusChem*, 2019, **12**, 3003.
61 S. Zhu, J. Qin, F. Wang, H. Li and L. Chu, *Nat. Commun.*, 2019, **10**, 749.
62 G. S. Lee, D. Kim and S. H. Hong, *Nat. Commun.*, 2021, **12**, 991.
63 (*a*) J. D. Nguyen, J. W. Tucker, M. D. Konieczynska and C. R. J. Stephenson, *J. Am. Chem. Soc.*, 2011, **133**, 4160; (*b*) N. Iqbal, S. Choi, E. Kim and E. J. Cho, *J. Org. Chem.*, 2012, **77**, 11383; (*c*) C. Yu, N. Iqbal, S. Park and E. J. Cho, *Chem. Commun.*, 2014, **50**, 12884; N. J. W. Straathof, S. E. Cramer, V. Hessel and T. Noel, *Angew. Chem., Int. Ed.*, 2016, **55**, 15549.
64 G.-R. Park, Y. Choi, M. G. Choi, S.-K. Chang and E. J. Cho, *Asian J. Org. Chem.*, 2017, **6**, 436.
65 D. P. Tiwari, S. Dabral, J. Wen, J. Wiesenthal, S. Terhorst and C. Bolm, *Org. Lett.*, 2017, **19**, 4295.
66 Y. Chen, J. Wang, X. Wu and C. Zhu, *ACS Org. Inorg. Au*, 2022, **2**, 392.
67 X. Nie, T. Xu, J. Song, A. Devaraj, B. Zhang, Y. Chen and S. Liao, *Angew. Chem., Int. Ed.*, 2021, **60**, 3956.
68 H. Cao, H. Jiang, H. Feng, J. M. C. Kwan, X. Liu and J. Wu, *J. Am. Chem. Soc.*, 2018, **140**, 16360.
69 (*a*) J. Muzart, *Eur. J. Org. Chem.*, 2010, 3779; (*b*) M. Hossain, U. Das and J. R. Dimmock, *Eur. J. Med. Chem.*, 2019, **183**, 111687; (*c*) S. Zhang, H. Neumann and M. Beller, *Chem. Soc. Rev.*, 2020, **49**, 3187.
70 M. Zhang, J. Xi, R. Ruzi, N. Li, Z. Wu, W. Li and C. Zhu, *J. Org. Chem.*, 2017, **82**, 9305.
71 Z. Lei, A. Banerjee, E. Kusevska, E. Rizzo, P. Liu and M.-Y. Ngai, *Angew. Chem., Int. Ed.*, 2019, **58**, 7318.

 This journal is © The Royal Society of Chemistry 2026

72 K. Liu and A. Studer, *J. Am. Chem. Soc.*, 2021, **143**, 4903.
73 J. Kim, S. Müller and T. Ritter, *Angew. Chem., Int. Ed.*, 2023, **62**, e202309498.
74 H. M. Ko, C. W. Lee and M. S. Kwon, *ChemCatChem*, 2023, **15**, e202300661.
75 (*a*) Q. Cheng, H.-F. Tu, C. Zheng, J.-P. Qu, G. Helmchen and S.-L. Yu, *Chem. Rev.*, 2019, **119**, 1855; (*b*) P.-S. Wang and L.-Z. Gong, *Acc. Chem. Res.*, 2020, **53**, 2841; (*c*) Y. Chen, Y. Yao and L. Shi, *Chem. – Eur. J.*, 2026, **32**, e03638.

Open Access Article. Published on 18 May 2026. Downloaded on 5/26/2026 2:04:15 AM.
This article is licensed under a Creative Commons Attribution 3.0 Unported Licence.